This is to certify that the

thesis entitled
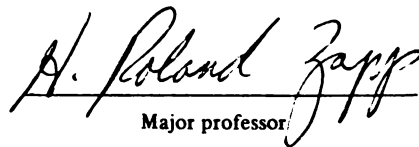
ULTRASONIC MEASUREMENT FOR HIGHLY ATTENUATED MATERIAL

presented by

Mo Zhang

has been accepted towards fulfillment
of the requirements for

_____MS_____ degree in __Electrical__ Engineering

Major professor

Date 4/7/94

PLACE IN RETURN BOX to remove this checkout from your record.
TO AVOID FINES return on or before date due.

DATE DUE	DATE DUE	DATE DUE
APR 2 8 2007	——————	——————
——————	——————	——————
——————	——————	——————
——————	——————	——————
——————	——————	——————
——————	——————	——————
——————	——————	——————

MSU Is An Affirmative Action/Equal Opportunity Institution
c:\circ\datedue.pm3-p.1

ULTRASONIC MEASUREMENT FOR HIGHLY

ATTENUATED MATERIAL

By

Mo Zhang

A THESIS

Submitted to
Michigan State University
in partial fulfillment of the requirements
for the degree of

MASTER OF SCIENCE

Department of Electrical Engineering

1994

ABSTRACT

ULTRASONIC MEASUREMENT FOR HIGHLY ATTENUATED MATERIAL

By

Mo Zhang

This paper describes the design of an ultrasonic measurement system and the use of ultrasonic detection to analyze the data from highly attenuated materials.When a fruit tree is damaged by borer infestation, the properties of the boundary between the bark and the trunk of the cherry tree change, and if the borer damage is extensive, large spatial separation occurs. The damaged areas contain a greater percentage of air space, feces, larvae or other low density substance. The boundary material property change inside the fruit tree can be detected by using ultrasonic measurements.

As a result, when an ultrasonic pulse propagates through highly attenuated damaged layers, preferential attenuation of high-frequency components cause the pulse to change in shape continuously as it propagates through the medium. The center frequency appears to shift toward the low-frequency end of the pulse, with a decrease in intensity as well. The effective frequency shift allows feature identification.

ACKNOWLEDGMENTS

I would like to express my greatest gratitude to Dr. H. Roland Zapp and Dr. Bong Ho, my advisors, for their guidance on this thesis and for my education and I would like to thank Dr. C.L. Wey for his helpful suggestions.

Furthermore, I also would like to express my gratitude to my wife, Jingchun Xu, for her support and taking care of our daughter during these years of my graduate study.

TABLE OF CONTENTS

LIST OF TABLES

LIST OF FIGURES

1.INTRODUCTION

Wood is an anisotropic (orthotropous) material and is highly attenuative. Consequently a significant component of ultrasonic research is concerned with determining the relationship between the physical and structural properties of wood and the propagation of the acoustic wave. The physical properties being investigated include the moisture content, density, and temperatures of wood. Structural properties include propagation direction(i.e., grain direction) and within ring growth pattern(i.e., diffuse) versus ring porous vessel distribution for hardwoods and abrupt versus gradual transition from early to late wood for softwood.

Preliminary investigations indicated that attenuation was influenced by moisture content and propagation direction, but the trends were not consistent (Lemaster and Dornfel 1987). In fact Lemaster and Dornfeld (1987) reported that if the measurements made on the oven-dry specimens were removed from the analysis, the data showed virtually no relationship between moisture content and signal energy. The determination of wood properties using acoustic wave propagation has attracted considerable research interest. Miller, et al. 1965, Shaw 1978, and Arita and Kuratani (1984) have used acoustically based nondestructive evaluation (NDE) devices to monitor the structural condition of wood utility poles subjected to the degradative effects of decay and insect attack. Patton-Mallory et al.(1987) used multiple waveform characteristics to distinguish decayed wood from nondecayed wood under controlled conditions in the laboratory. More recently, ultrasonic analysis has moved into a subsequent stage of multiparameter analysis of the transmitted waveform in both the time and frequency domain, Beall. (1988).

1

The use of ultrasonic pulse-echoes to detect damage, such as borer infestation, inside fruit trees has not previously been attempted. Therefore, the purpose of this thesis is to develop and evaluate an ultrasonic detection device for borer damage in Michigan cherry trees. When an incident pulse reaches a boundary between two different media, such as the cambium between the trunk and the bark of the cherry tree, the amount of wave energy which is reflected or refracted is dependent on the acoustic impedance at the boundary. The amplitude of the reflected signal provides information on the acoustic impedance of the target. A tree damaged by the borer will contain air, feces, and larvae in the damaged areas which results in a higher acoustic impedance mismatch relative to the normal interface between bark and the trunk of the fruit tree. Thus, at an interface between the bark and the damaged areas, the reflection coefficient approaches unity, and an incident pulse is essentially reflected with negligible energy transmitted through the damaged area. Measurement of the reflected or transmitted energy in the time domain can therefore be used to indicate the presence of borer damage to the fruit tree.

The measurements in the time domain are conventional applications of ultrasonic nondestructive testing, when evaluation is based primarily upon amplitude and time information. The transducer is selected to satisfy a nominal test frequency that meets the requirements of the inspection task, but, in general, the relationship between the initial and received pulse spectrum is not recorded.

The differences between borer and non-borer-damaged samples identified from reflected signals are more readily quantified if the frequency content of reflected signals is determined. This is achieved by carrying out a Fourier transform of the reflected signal. At any time and for any component, the time and frequency-domain can be interchanged by Fourier or inverse Fourier transform. In the time-domain, the signal is sufficiently de-

scribed by its amplitude while in the frequency domain both amplitude and phase are required.

This thesis discusses both techniques to characterize the borer-damage inside the cherry tree. The power spectrum of the reflected signal from a borer damaged and non-borer-damaged sample is compared to see their differences at different frequency components. This application will be illustrated by laboratory results obtained with a detection system now being used in a program aimed at evaluating the utility of spectral analysis in many different areas.

The acoustic attenuation coefficient measured in dB/cm is known to increase linearly with frequency for most highly attenuated material. The slope of this linear function is denoted by the symbol β. The effect of this acoustic attenuation on an ultrasonic pulse having a Gaussian envelope is to translate the normalized power spectrum to lower frequencies by an amount, ∇f, proportional to β while maintaining the bandwidth. If the medium has a loss factor which can be described by $H(f) = \exp((-\kappa|f|^p)x)$, where f is the frequency and $o \leq p \leq 2$ (valid for tissues and other objects of interest), then the pulse retains its Gaussian shape, shifting only its center frequency (L. Ferrari, 1986). The difference between borer damaged and non-borer damaged samples is manifested in a frequency shift observed in the spectrum of the reflected pulses. In particular the power spectrum of the reflected signal from the damaged layer is shift to lower frequency by an amount ∇f. Thus, analysis of the spectral composition or frequency shift at given frequencies provides the potential for distinguishing between borer and non-borer damaged samples. This capability is of major importance in helping to identify which cherry tree are borer infested and then need to be separated and removed.

In this thesis, the ultrasonic detection system and experimental set up are described. The ultrasonic principles which are concerned with understanding the dynamics of the propagation of ultrasonic pulses in material, and the influence of boundary damage on the return signal are reviewed. It is hypothesized that the difference in signal return from borer and non-borer-damaged material could be exploited to image the damage distribution inside tree trunks. A mathematical model is established using both time domain signal analysis and frequency-domain analysis. The experimental results are presented to show validity of the theoretical development and lead to the conclusions that the detection of borer-damage is indeed possible. Throughout this paper it is assumed that broad-band sources are used.

2.THE MEASUREMENT SYSTEM AND EXPERIMENTAL METHODS

2.1 Description of the System

It is convenient, for purpose of description, to consider the ultrasonic detection system as two distinct part, the scanning system and the signal processing unit. In this section each part will be described individually.

The function of the scanning system is to use ultrasonic techniques to collect and store information related to defects or damage from a given area of a specimen, so that the signal processing unit can use it to construct a visual representation of that specimen and of any defects present. The information collected is, therefore, concerned with the size and position of areas of ultrasonic reflectivity within a testing material. These areas are boundaries between media of different acoustic impedances and the reflectivity is a measure of the mismatch in acoustic properties. The data are obtained by recording the data at equally spaced positions over the surface of the material to be examined. At each position the ultrasonic waveform reflected from the specimen is digitized and information concerning the time and amplitude of echoes, along with the X and Y position co-ordinates, is stored.

When ultrasonic techniques are used to detect defects, information is conventionally collected and displayed in three basic ways, called A-, B- and C-Scans. Because the program for detecting borer-damage inside the fruit tree is just concerned with the A-Scan mode, only this will be described. An A-Scan shows the amplitude of echoes or reflections

viewer with information concerning the depth and reflection of points of discontinuity in the material below the sample at one location. By keeping the sample and transducer under water a good acoustic coupling between the two is achieved. A three dimensional image can be generated by computer controlled stepper motors for X and Y positioning while the Z position is obtained by A-Scan ranging. At each position the ultrasonic waveform reflected from the sample is digitized and information concerning the time and amplitude of echoes, along with the X and Y position co-ordinates, are stored. After the data is sampled, it is sent to the signal processing unit for further use.

A schematic diagram of the experimental equipment used is shown in Figure 2.1. The detection system consisted of an IBM-PC-486 Microcomputer, an Ultrasonic 5050 Pulser/Receiver Unit (P/R unit), a Waveform Acquisition and Arbitrary Generator (WAAGII) board, an Accuscan Immersion Transducer, and the MD-2 Dual Stepper Motor Driver System.The IBM-PC-486 Microcomputer is the core of the system. Each of the elements of the system are peripherals of the computer in that they are controlled by the signal initiated by the computer. It features a 64K high speed cache and 4Mb RAM. The microcomputer is used to both to control the scanning equipment and the signal processing system. The transmission and reception of the ultrasonic wave is achieved using a commercial ultrasonic transducer and pulser/receiver unit. The Model 5050 is a broadband ultrasonic pulser/ receiver unit that, when combined with appropriate transducer, provides a unique, low-cost ultrasonic measurement capability. The WAAGII board converts a preselected portion of a time varying analog waveform to digital (binary) data with maximum sample frequency for a single channel (40 MHz to acquire, display and store waveform as a function of time) which is equivalent to distance, if a value for the velocity of sound in the medium is known.

```
┌──────────────────┐
│ PULSER / RCEIVER │
└──────────────────┘
```

DISTILLED WATER

IBM PC-486-25 MHz MICROCOMPUTER

STEPPER MOTOR

MD-2 DUAL STEPPER MOTOR DRIVER SYSTEM

IBM GRAPHICS PRINTER

WAAGII BOARD INCLUDE A/D CONVERTER WITH SAMPLING AT 40 MHZ AND THEN PUTING IT INTO RAM

NO

END OF SAMPLE?

YES

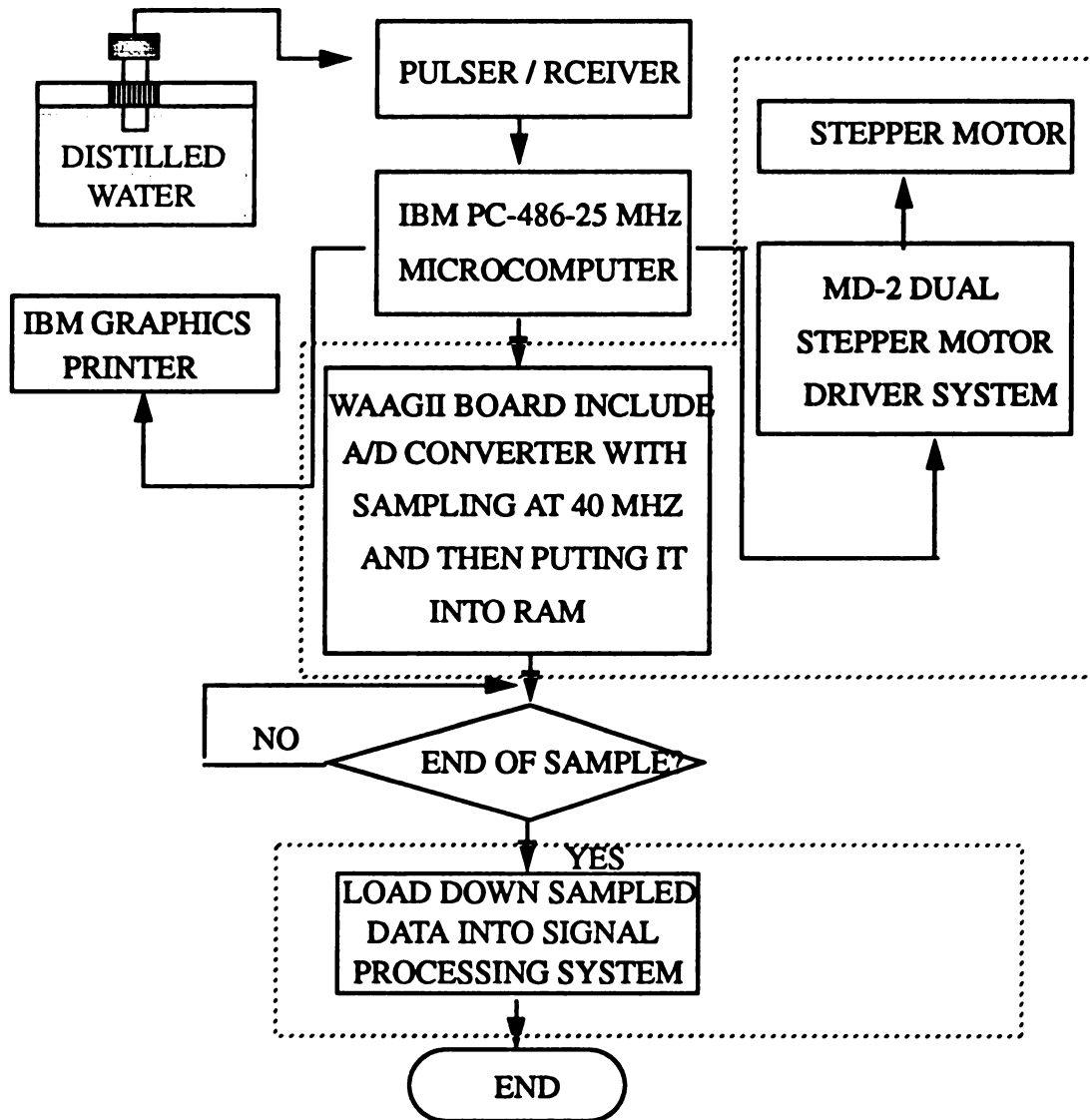LOAD DOWN SAMPLED DATA INTO SIGNAL PROCESSING SYSTEM

END

Figure 2.1 Schematic Diagram of the Experimental System

The A-Scan presents the amplitude and period. The MD-2 Dual Stepper Motor Driver System consists of MD-2Dual Stepper Motor Controller, XY-18 Positioning Table, and two Stepper Motors. Motors can be driven using the keyboard and position information can be saved to the disk of the microcomputer for complicated motion sequences.

During scanning, both the specimen and transducer are kept under water in an immersion tank to ensure good acoustic coupling between the two. The transducer is held above the specimen, the exact height being determined by the focal length of the transducer. The transducer is moved parallel to the surface of the material by two stepper motors which control movements in the X and Y directions.

Before scanning commences, the co-ordinate system is set up by the operator. Using a keyboard to control its position the transducer is moved to an arbitrary location in the immersion tank, remote from the specimen, which is then defined as the co-ordinate origin. The area of the specimen to be scanned or the one point of the specimen to be sampled (for our experiment) is then selected by moving the transducer to that location. The co-ordinates of the scan area are defined in terms of numbers of pulses to the stepper motors. These units are related to conventional units by the step size of the motors, which is 0.1 mm/step. The operator also defines the spatial resolution by specifying the intervals at which measurements will be recorded, the minimum spacing being 0.1mm.

Once the initial parameters have bee set, the sampling starts. A trigger pulse is sent to the P/R unit, which itself generates an electrical pulse to excite the ultrasonic transducer. This pulse is converted by the transducer into an ultrasonic wave packet, which propagates towards the specimen. The wave reflects from boundaries and discontinues within the material, returns to the transducer and is processed by the signal processing unit. Each

time the P/R unit is triggered in this way, the resultant A-scan waveform is available at its signal output, after any required analog processing has been performed.

The function of the data processing unit is to process the data stored during the scanning or sampling process and to display the results on a color monitor. The WAAGII board is used to digitize this signal. It measures the amplitude of the signal at equally spaced sample points in time using an 8 bit analog-to-digital converter. This provides a digital equivalent of the input voltage as one of 256 amplitudes at each sample time. The WAAGII board is inserted into PC-mother board and is externally controlled by the PC-486 microcomputer.

The WAAGII board starts recording and digitizing a waveform only after it has received a trigger pulse. This pulse is produced by the P/R unit when it sends the excitation pulse to the transducer, and hence is synchronized with the ultrasonic waveform. However, there is relatively long delay between the transducer excitation pulse and the first reflected echo from the specimen surface due to the time taken for ultrasound to travel through the water. Since the transient WAAGII board will only record a finite number of samples, a variable delay is introduced between the trigger output of the P/R unit and the trigger input of the transient WAAGGII board. This time delay is adjusted before scanning or sampling, so that the trigger arrives at the transient WAAGII board to start it recording just before the signal corresponding to the first reflected echo arrives at the signal input.

The waveform to be digitized comprises a peak due to the main electrical pulse from the P/R unit, a specimen front surface echo, and possibly other echoes representing the back surface and defects within the material. Once the waveform has been digitized, the amplitude of each sample point is stored in the computer. To reduce the effects of random noise a number of waveforms can be averaged. This is done by digitizing a specified

number of A-scan waveforms and adding their amplitude values at corresponding sample times. These summed values are then used in the subsequent processing.

The software compares the amplitude of each sample with preceding values and detects any peaks. Once a peak has been found approximately its position is then computed accurately, and its amplitude determined. The amplitude is then divided by the number of A-scan waveforms summed together to complete the averaging operation and the information stored. Any further peaks are found in the same way.

When the A-scan information from the first measurement point on the specimen's surface has been stored, the computer sends out a series of pulses to advance the stepper motor of the transducer transport mechanism to the next data point. The P/R unit is triggered to initiate the next ultrasonic pulse so that the whole process can start once again.

2.2 Experimental Procedures

Conventional ultrasonic pulse-echo system are widely used to detect the defects inside materials. These systems transmit short bursts of radio frequency ultrasound into the test object and display the echoes reflected from inhomogeneities on a microcomputer. The time of occurrence and amplitude of these echoes can be related respectively to the location and magnitude of the ultrasound reflectors. To avoid range ambiguities in systems that transmit the same waveform in each burst, it is necessary to wait until the echo from the most distance target has returned before another burst can be transmitted. Therefore, the repetition period T of the rf bursts is limited by

$$T \geq (2R_{max})/c \qquad (2.1)$$

where c is the velocity of ultrasound and R_{max} the maximum range from which echoes can be detected.

The testing signal was generated from a 2.25MHz, 1.5 cm diameter ultrasonic transducer with a 5 cm focal length. The panametrics 5050 Pulser/Receiver was employed to provide the pulse signal to the transducer and to receive the reflected signals. The ultrasonic reflected waveform was sampled by the WAAGII board with a high sampling rate of 40MHz. The sampled data were sent to an IBM-PC-486-25MHz microcomputer for signal processing. After recording the reflected signal from the non-borer-damaged sample, the target was replaced with a borer-damaged sample and the measurements repeated.

The impulse response, and its frequency spectrum, of the reflected signals from borer damaged samples are compared with that of the impulse response and spectrum, with the same distance between the transducer and the surface of the sample. For the target that is known to be non-borer-damaged data are stored in the computer can be used to carry out the comparison to non-damaged targets in order to give an immediate indication of the damage level.

There were 11 cherry tree samples used in our tests which were obtained from operating fruit farms in Northwest Michigan. To evaluate whether a difference exists between damaged and non-borer-damaged samples, we cut two similar diameter (12 cm diameter) fruit tree 20 cm bolts, one borer-damaged and the other non-borer-damaged. In order to minimize the scattering of the ultrasound signal from the non-uniform bark and to provide a perpendicular signal, we scrapped the bark to provide a flat surface.

The pulse-echo technique generally uses a single transducer capable of sending and receiving a pulse of ultrasound. The delay between pulses and the geometry of the transducer ensure that reverberations from the transmitting crystal have died away before

the echoes are received. Provided the pulses are short enough the individual echoes from each interface can be resolved, their position and amplitude being used to detect the presence of borer-damaged areas. A large proportion of ultrasound will be reflected at a borer-damage area owing to its large reflection coefficient. Echoes from discontinues behind the borer-damaged area will be reduced and usually disappear.

Due to the severe impedance mismatch between solid material and air, it is difficult to propagate ultrasound from a transducer through air to the testing sample surface. It is therefore vital that there be a satisfactory coupling agent between the transducer and the test samples. This was achieved by immersing the test samples and the transducer in a water tank. The transducer can be independently positioned along three dimensions. The distance between the transducer and the surface of the sample was adjusted by a sliding transducer-holder.

The borer-damaged area usually occurs just below the boundary between the bark and the trunk, and forms a very thin damaged layer, as the larvae forms tunnels through the soft cambium layer. A borer-damaged sample, with its borer-damaged layer perpendicular to the incident signal, was selected for testing and a non-damaged sample of similar shape and size was used for comparison.

3. THEORETICAL BACKGROUND

Propagation of ultrasound in wood material depends on the ultrasound propagation velocity, the acoustic impedance, the attenuation in the wood and scattering of ultrasound by the inhomogeneities in the wood structure. It is obvious that there is a considerable amount of information contained in an ultrasonic wave propagated through wood. Thus, in order to extract the information about variation of acoustic impedance along the path of propagation, the object is modelled as consisting of parallel layers of different impedances. Some basic properties of ultrasound propagation are employed for this purpose.

3.1 The Characteristic Acoustic Impedance

The ratio of the acoustic pressure to the particle velocity in a medium is defined as the specific acoustic impedance for that medium. For plane wave in free field conditions it can be show that this quantity is equal to the product of the density of the medium (ρ) and the velocity of sound (c) in the medium, which is known as the characteristic acoustic impedance for that medium (Z), or

$$Z = \rho c \tag{3.1}$$

The extent to which ultrasonic energy is transmitted or reflected at an interface separating two continuous isotropic media is determined by the characteristic impedance. The relationship between pressure and particle speed for the forward wave is

$$P_1\left(t - \frac{x + k_1}{c}\right) = ZU_1\left(t - \frac{x + k_1}{c}\right) \tag{3.2a}$$

13

and for the backward wave

$$P_2\left(t + \frac{x + k_2}{c}\right) = -ZU_2\left(t + \frac{x + k_2}{c}\right)$$ (3.2b)

where U_1 and U_2 represent forward and backward traveling waves, respectively, propagating at velocity c and k_1, k_2 are real constants and P_1, P_2 represent the acoustic pressure.

3.2 Reflection and Transmission at an Interface

When an ultrasonic plane wave meets a boundary between two different media it may be partially reflected. The ratio of the characteristic impedance of the two media determines the magnitude of the reflection coefficient at the interface. The reflected wave is returned in the negative direction through the incident medium at the same velocity with which it approached the boundary. The transmitted wave continues to move in a positive direction, but at a velocity corresponding to the propagation velocity in the new medium. Just as optics, Snell's law for reflection applies, and the angles of incidence and reflection are equal when the wavelength of the ultrasound is small compared to the dimensions and roughness of the reflector as illustrated in Figure 3.1

In Figure 3.1 the subscripts i, r and t refer to the incident reflected and transmitted waves respectively and 1 and 2 to the first and second media that the ultrasound encounters. With the ultrasonic plane wave traveling in the direction θ_i relative to the Z-axis, a distance S in the direction of propagation may be related to its X and Z components by
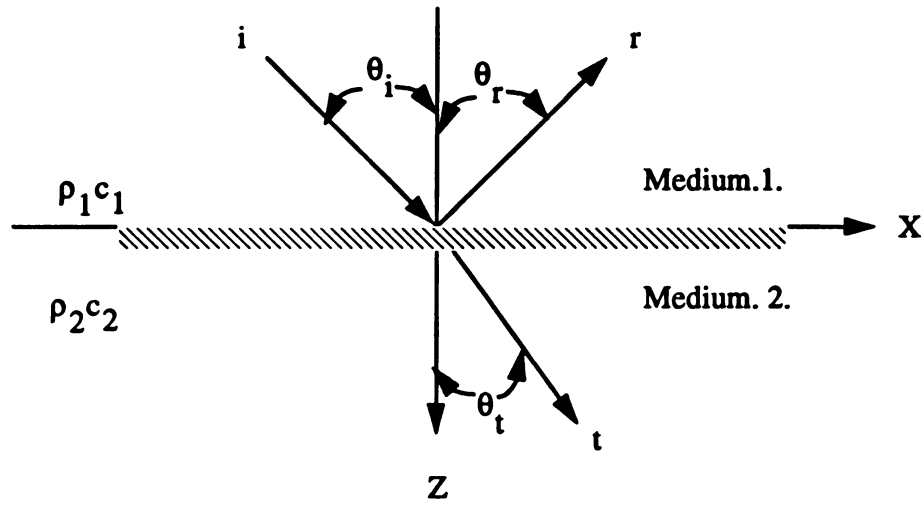
$$S = x\sin\theta_i + z\cos\theta_i$$ (3.3)

Figure 3.1 Reflection at an Interface

Therefore, the incident pressure plane wave in complex notation becomes

$$P_i(t, x, z) = A_1 \exp\left\{ j\omega\left[t - \frac{x\sin\theta_i + z\cos\theta_i}{c_1} \right] \right\}$$

(3.4a)

Similarly, the reflected and transmitted pressure waves are

$$P_r(t, x, z) = B_1 \exp\left\{ j\omega\left[t - \frac{x\sin\theta_r + z\cos\theta_r}{c_1} \right] \right\}$$

(3.4b)

$$P_t(t, x, z) = A_2 \exp\left\{ j\omega\left[t - \frac{x\sin\theta_t + z\cos\theta_t}{c_2} \right] \right\}$$

(3.4c)

At the medium boundary, the pressure must be continuous. Thus

$$P_i + P_r = P_t \qquad \text{(at } z=0) \qquad (3.5a)$$

or

$$A_1 \exp\left(\frac{-j\omega x \sin\theta_i}{c_1}\right) + B_1 \exp\left(\frac{-j\omega x \sin\theta_r}{c_1}\right) = A_2 \exp\left(\frac{-j\omega x \sin\theta_t}{c_2}\right) \qquad (3.5b)$$

Two results from optics are helpful in defining the relationships among the incident, reflected and transmitted waves at the boundary between two media. First, the angle of reflection is equal to the angle of incidence, that is

$$\theta_r = \theta_i \qquad (3.6)$$

Second, Snell's law relates the angles of incidence and transmission in terms of the speed of sound in the two media. For the angles as defined in Figure 3.1 Snell's law requires that

$$\frac{\sin\theta_i}{c_1} = \frac{\sin\theta_t}{c_2} \qquad (3.7)$$

Applying these relationships to (3.5b), we see that

$$\frac{\sin\theta_i}{c_1} = \frac{\sin\theta_r}{c_1} = \frac{\sin\theta_t}{c_2} \tag{3.8}$$

with the result that all exponents in (3.5.b) are equal. Therefore, we again obtain

$$A_1 + B_1 = A_2 \tag{3.9}$$

As an additional boundary condition, we require that the particle velocity in the z-direction be continuous. This results in the relationship

$$U_i\cos\theta_i + U_r\cos\theta_r = U_t\cos\theta_t \tag{3.10}$$

where

$$U_i = \frac{A_1}{Z_1}$$

$$U_r = \frac{B_1}{Z_1}$$

$$U_t = \frac{A_2}{Z_2}$$

sing equations (3.6) and (3.9) in (3.10), we obtain:

$$(U_i - U_r)\cos\theta_i = U_t\sin\theta_t \tag{3.11}$$

The amplitude of the reflected and transmitted pulses are dependent on the reflection coefficient of the interface, which may be calculated by solving for the ratio of reflected to the incident amplitude

$$\frac{P_r}{P_i} = \frac{B_1}{A_1} = \frac{Z_2\cos\theta_i - Z_1\cos\theta_t}{Z_2\cos\theta_i + Z_1\cos\theta_r} \tag{3.12}$$

The ratio of the transmitted to incident pressure amplitude gives the following result

$$\frac{P_t}{P_i} = \frac{A_2}{A_1} = \frac{2Z_2\cos\theta_i}{Z_2\cos\theta_i + Z_1\cos\theta_t} \tag{3.13}$$

For normal incidence,

$$\theta_i = \theta_r = \theta_t = 0 \tag{3.14}$$

Thus from equations (3.12) and (3.13), the reflection coefficient R_{12} for normal incidence is:

$$R_{12} = \frac{P_r}{P_i} = \frac{Z_2 - Z_1}{Z_2 + Z_1} \tag{3.15}$$

and the transmission coefficient is

$$T_{12} = \frac{P_t}{P_i} = \frac{2Z_2}{Z_2 + Z_1} \tag{3.16}$$

According to equations (3.14) and (3.15), no phase shift occurs between the incident wave and the transmitted wave either in the displacement or in the stress, regardless of which medium has the higher acoustic impedance. However, when the acoustic impedance of medium 2 is greater than that of medium 1, the displacement of the reflected wave is 180^0 out of phase with that of the incident wave, but the stresses are in phase. The reverse is true if the acoustic impedance of medium 2 is less than that of medium 1.

In practice, the actual situations are often considerably more complicated than the ideal conditions described here. Reflections and refraction at interfaces between media enter into every aspect of the applications of ultrasonic energy.

3.3 Attenuation of an Ultrasonic Wave

The intensity of a plane progressive ultrasound field can be reduced by interaction with the transmitting medium. Two important sources of attenuation are scat-tering and absorption. The interface of each discontinuity within a medium serves as a reflecting surface, the size of which (in relation to the wavelength) determines its effect as scatterer. Most of this scattered energy no longer moves only in the original direction of propagation and thus the total amount of energy transmitted is reduced. When scattering occurs, the amplitude of the scattered signal is proportional to f^n where f is the frequency of the ultrasound signal and n is greater than or equal to 1. Thus greater scattering occur at higher frequencies.The other significant source of attenuation is absorption, which occurs primarily at the macromolecular level for logitudinal waves (Carstensen, 1979; Edmonds, 1981). The attenuation coefficient is always larger than the absorption coefficient because absorption is only one of the means by which the ultrasound field is attenuated.

Attenuation refers to the diminishing of intensity of a waveform as it progresses through a medium. The effect of attenuation on a periodic wave is demonstrated by the equation:

$$P = P_0 e^{-\alpha x + j(\omega t - kx)} \tag{3.17}$$

where P_0 is the pressure amplitude of the wave as it leaves the source, $k = \omega/c$, is the propagation constant and α is amplitude attenuation coefficient of the medium for a given frequency. Two important source of attenuation coefficient α are scattering and absorption. It can be expressed by $\alpha = \alpha_a + \alpha_s$, where α_a is absorption coefficient and α_s is scattering coefficient (Chivers, 1980). Upon encountering an infinite plane surface that is parallel to the front, part of the energy is reflected, depending on the relationship between acoustic impedances of the two media. During the reflection process, the wave also may undergo a 180^0 shift in phase. If the distance between the source and the reflecting surface is L, the pressure amplitude of the incident wave at L is

$$P_i = P_0 e^{-\alpha L} \tag{3.18}$$

The pressure amplitude of the reflected wave at L is

$$P_r = P_0 e^{-\alpha L - 2\alpha_0 - 2j\beta} \tag{3.19}$$

where α_0 accounts for the loss of energy on reflection and β is the phase shift due to reflection.(β can be 0 or 90^0).

It is a measure of the rate at which an ultrasonic wave decreases in intensity by other than

geometric means as a function of distance it propagates through a medium. Since acoustic intensity is proportional to the square of acoustic pressure, this can also be expressed in terms of intensity I as:

$$I_x = I_0 e^{-2\alpha x} \tag{3.20}$$

where x is the distance traveled, and α is the amplitude attenuation coefficient.

Ultrasonic attenuation in a medium generally increases with increasing frequency in a manner that can be expressed approximately (over a limited frequency range) in the form:

$$\alpha = \alpha_0 f^n \tag{3.21}$$

where α is the amplitude attenuation coefficient of the medium at frequency f and α_0 is the attenuation coefficient of the medium at the reference frequency f_0.

4.TIME AND FREQUENCY DOMAIN ANALYSIS

4.1 Impulse Response

Determination of the difference between the borer-damaged and non-borer-damaged cherry tree depends on distinguishing the different acoustic impedances in the time domain. Ultrasonic impediography is based on the time domain characterization of the object in terms of an impulse response. This approach utilizes the incident and reflected signals to obtain the object impulse response which is then summed to give the impedance variation along the path of propagation. In the sampled data system, a signal can be described by a succession of impulse responses obtained by the reflections from various boundaries. The amplitude of reflected signal is an indication of the intensity of energy present in the reflected signal.

However, the reflected intensity is a complicated function of many other interface parameters such as:

1. Amount of attenuation in the path between the transducer and interface.

2. Angle that the axis of the ultrasound beam makes with the reflection interface.

3. Acoustical properties of the medium forming interface.

4.Curvature of the interface

5. Scattering properties of the interface.

This paper will assume that the attenuation can be accounted for by an exponential factor, although there are still four other factors that affect the intensity of the reflection. Approximating the discontinuity to be a smooth semi-infinite plane reduces the number of significant parameters of the reflection coefficient and of the angle of incident, which is define angle between the axis of the ultrasound beam and the normal to the incident.

The response of the detection system depends on the acoustic impedance of the testing material. A non-borer-damaged sample shows high stiffness relative to the borer-damaged one and thus damps the vibrations of the active transducer throughout the active band of frequencies. Any borer-damaged area in the cherry tree affects its impedance, which is reflected in the response of reflected signal from the interface between bark and trunk. Even voids, inclusions, and other perhaps non-serious defects cause changes in the spectrum that are identifiable. The curved boundaries inside the cherry tree between the bark and trunk can be minimized by using narrow ultrasonic beams which insure that the curvature displacements are much smaller that the illumination wavelengths. Spectral analysis of echoes from these boundaries can establish relative acoustic impedance differences and absorptivity as a function of frequency.

Although the cherry tree structures are acoustically complex, they can be thought of as a homogeneous material for a small thickness such as bark or multiple layers consisting of bark, damage area and trunk or just bark and trunk for non-damaged trees. The extent of the lateral area covered by the ultrasonic beam can be reduced by beam focussing. Hence the models shown in Figure 4.1a, Figure 4.1b, Figure 4.2a and Figure 4.2b can be used to represent the borer and non-borer-damaged cherry tree structures.
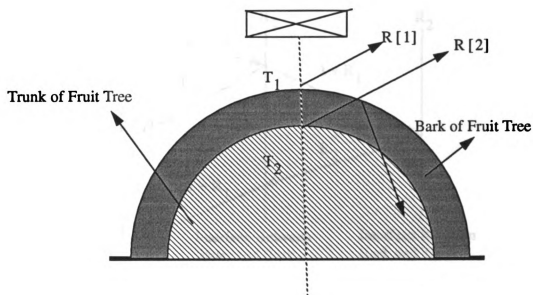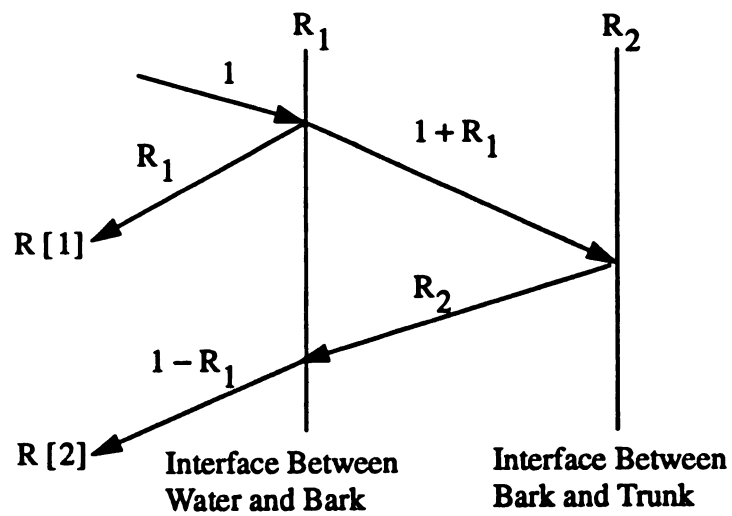
Figure 4.1a Non-Borer-Damaged Sample

Figure 4.1b Impulse Response of Layered Structure
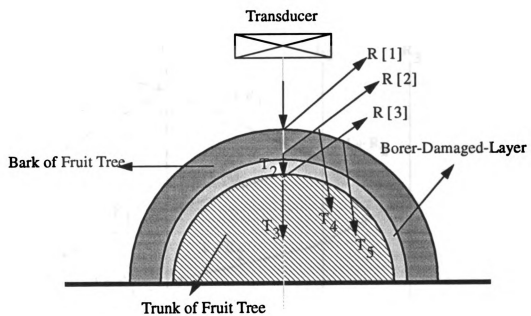for a Non-Borer-Damaged Sample
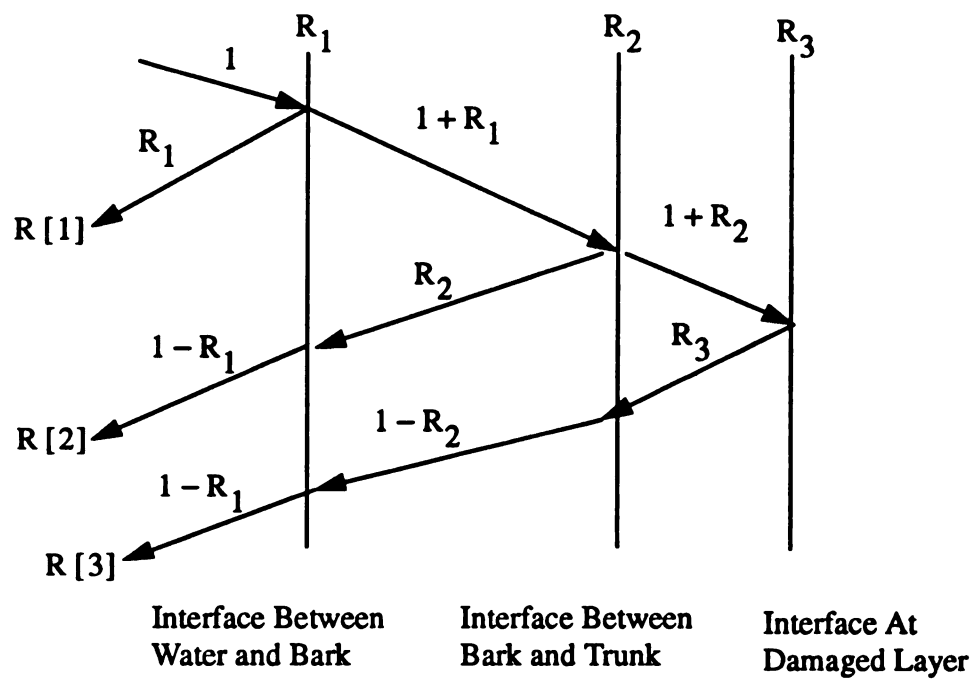
Figure 4.2a Borer Damaged Sample

Figure 4.2b Impulse Response of Layered Structure
for a Borer Damaged Sample

If the reflected signal is represented by R [k] , and the impulse response by h [n] , then:

$$h[n] = \sum_{k=1}^{\infty} R[k]\,\delta(n-k) \tag{4.1}$$

where

$$R[1] = R_1$$

$$R[2] = (1+R_1)R_2(1-R_1)$$

$$R[3] = (1+R_1)(1+R_2)R_3(1-R_1)(1-R_2)$$

$$R[k] = \prod_{i=1}^{n-1} R_n(1-R_i^2) , \tag{4.2}$$

where R_n is the reflection coefficient from the nth layer and the is the $\delta(n)$ is the dirac delta function (Lighthill.1958).

First, we consider the case of normal or perpendicular beam incidence on the non-borer-damaged cherry tree sample (Figure 4.1a and Figure 4.1b). By placing the sample in a water medium, most of the incident wave energy is reflected from the first boundary due to the large acoustic impedance mismatch between the cherry tree and the water interface. This should produce a negative reflection coefficient. The second much smaller

reflection R [2] comes from the interface between the bark and the trunk with intact cambium which should produce a positive echo. Since the signal is highly attenuated in the bark medium the resultant amplitude response is lower than anticipated. The impulse response from a non-borer-damaged sample is given by:

$$h[n] = R[1]\delta(n-1) + R[2]\delta(n-2) = R_1 + R_2(1-R_1^2) \qquad (4.3)$$

The experimental reflection results from non-borer damaged cherry tree sample are shown in Figure 4.3.

When the cherry tree is damaged by borer infestation, the borer-damaged areas are just under the bark in the cambium area. The borer-damaged areas are actually voids formed by the feeding consumption of cambium (see models shown in Figure 4.2a and 4.2b). Because of this, the acoustic impedance mismatch at the borer-damaged interface is much larger causing most of the wave energy to be reflected. As a result, the signal from the borer-damaged samples contains an additional reflection R [3] , from the bottom of the borer-damaged layer as shown in Figure 4.4. For the borer-damaged sample, the impulse response is represented by:

$$h(n) = R[1]\delta(n-1) + R[2]\delta(n-2) + R[3]\delta(n-3) = R_1 + R_2(1-R_1^2)$$

$$+ R_3(1-R_1^2)(1-R_2^2) \qquad (4.4)$$

Accurate determination of the impulse response function plays a critical role in ultrasonic detection systems. The impulse response is determined and the frequency response is computed with aid of a digital microcomputer which allows noise reduction and appropriate signal processing.
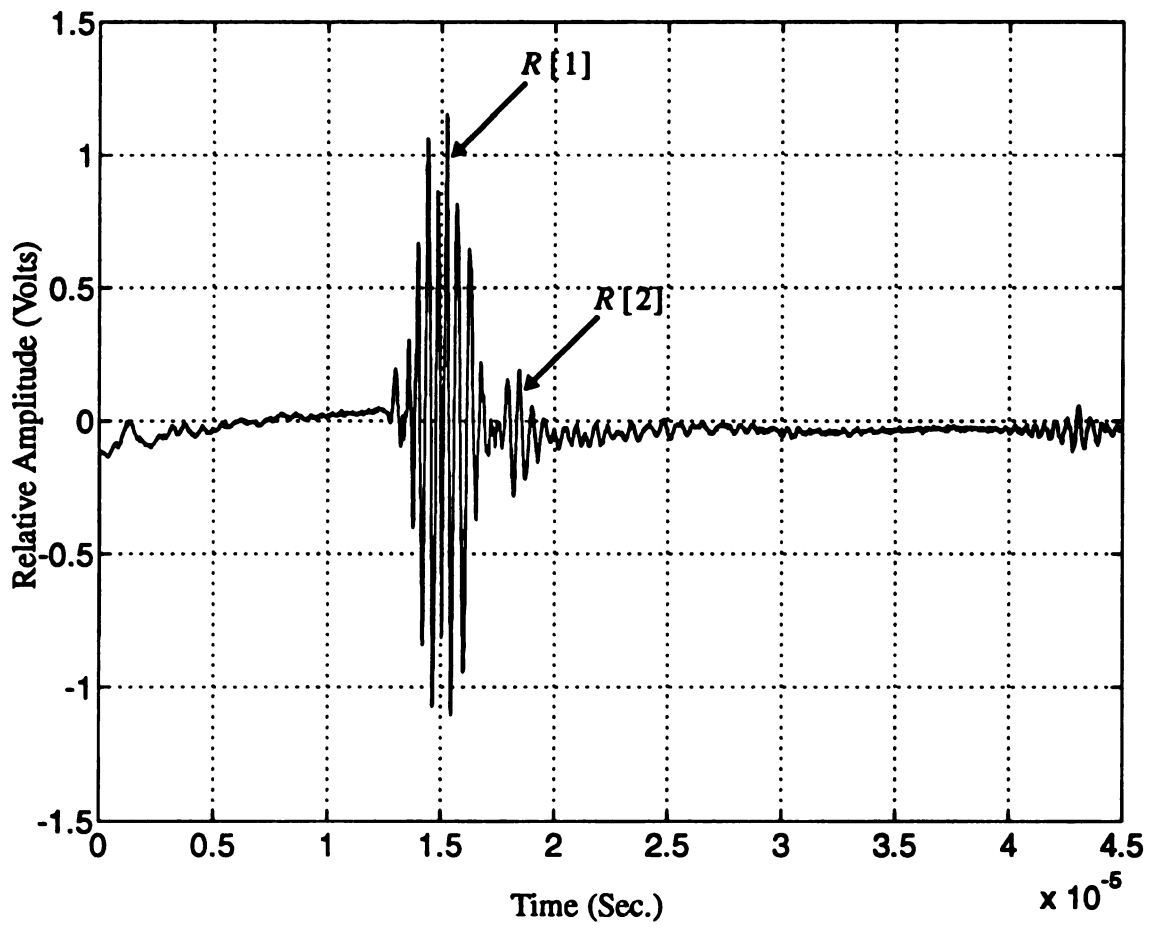
Figure 4.3 The Reflected Signal from a Non-Borer-Damaged Sample
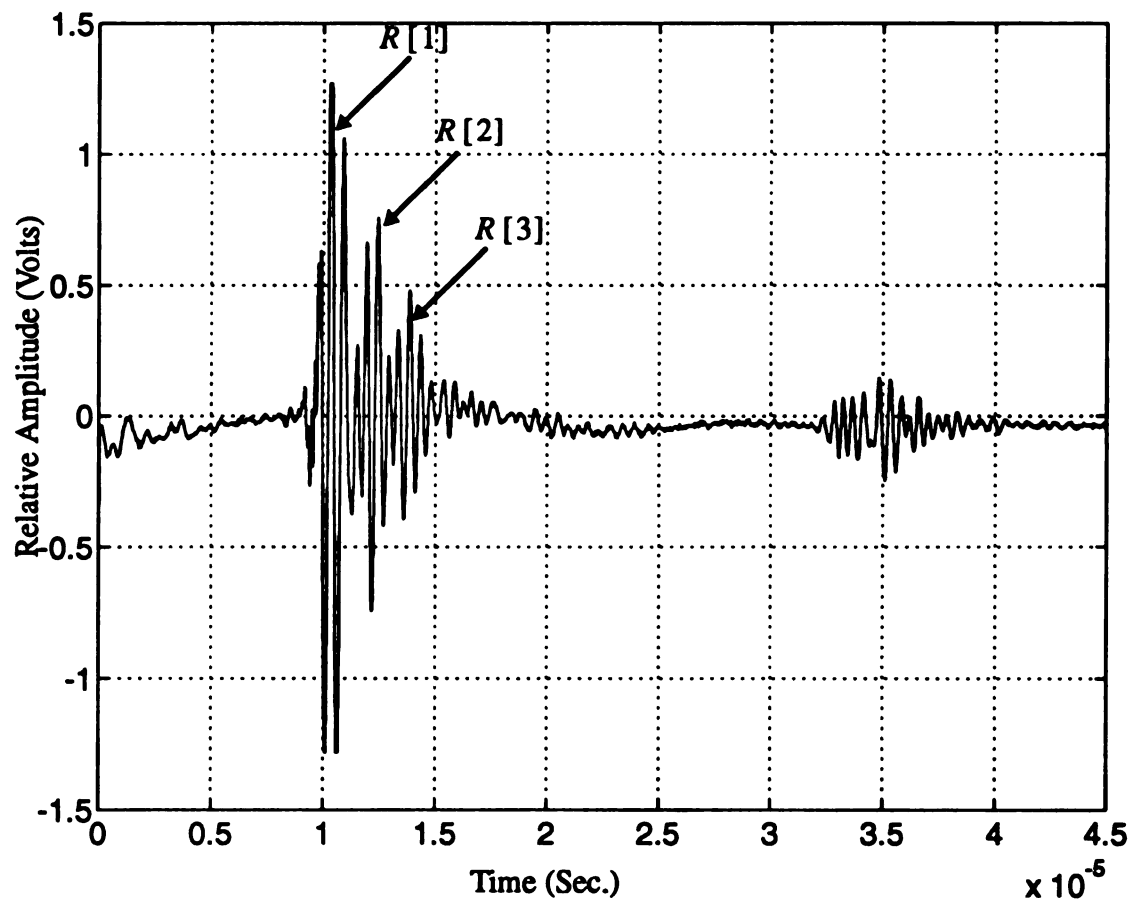
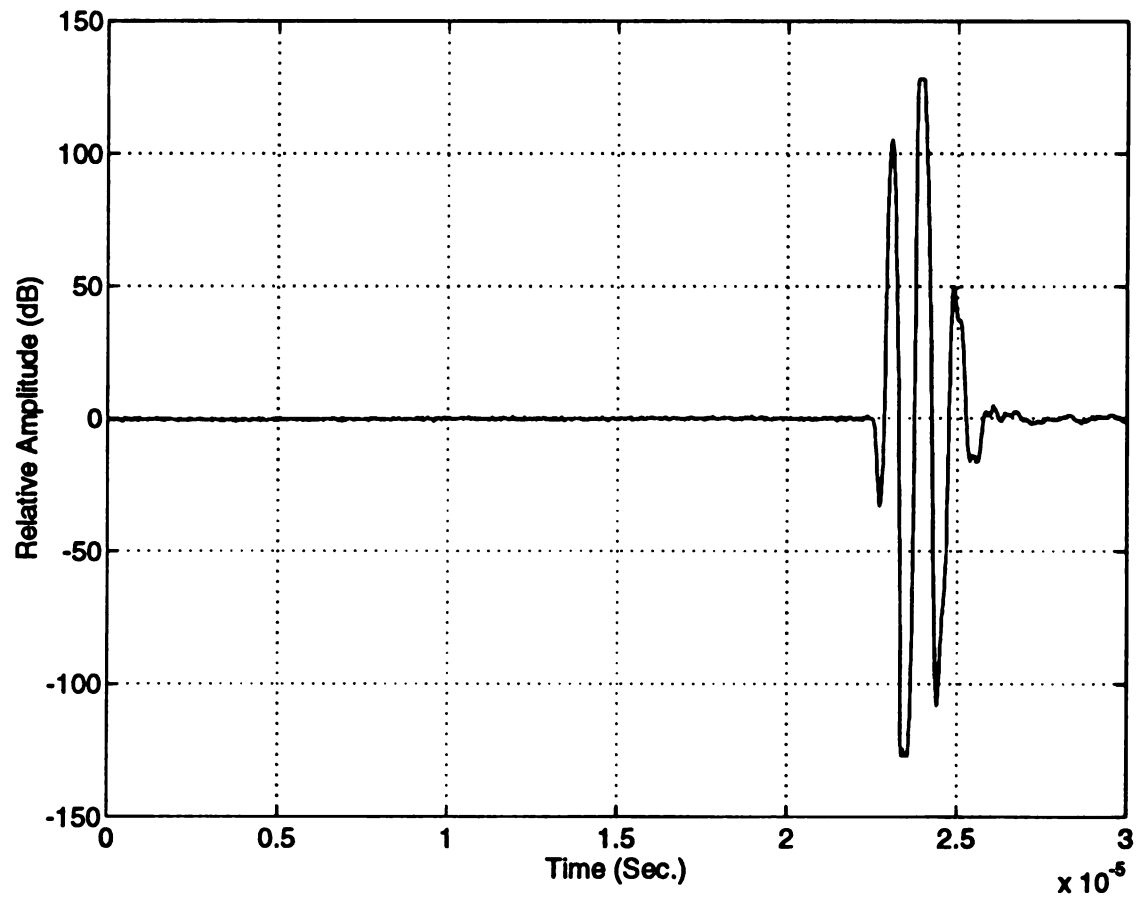Figure 4.4 The Reflected Signal from a Borer Damaged Sample

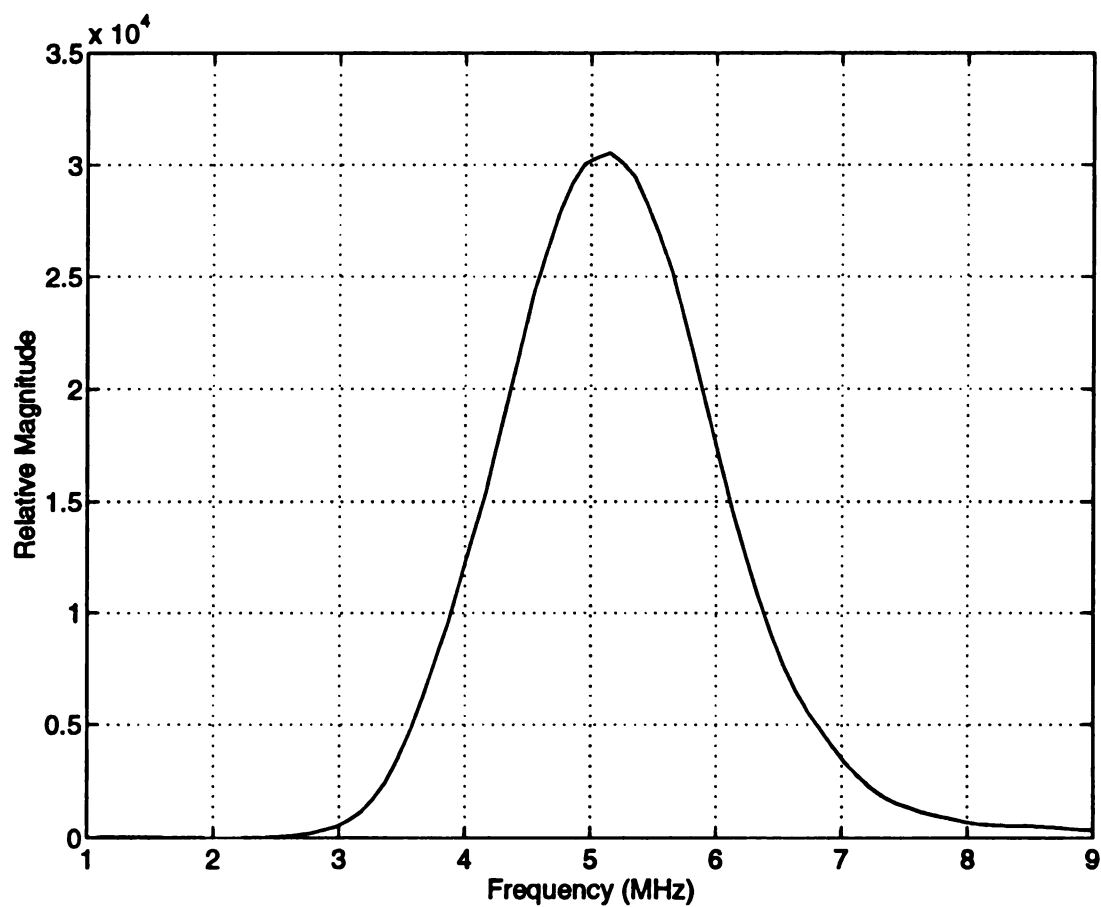Figure 4.5a The Reflected Signal from the Surface of a Wood Slab

Figure 4.5b The Power Spectrum of the Reflected Signal from the
Surface of a Wood Slab

Consider the response of a linear time-invariant system to an input signal of a unit impulse, or more generally to a sequence of impulses given by:

$$X(t) = \sum_{n=1}^{N} a_n \delta(t - t_n) \tag{4.5}$$

The output signal is, therefore,

$$y(t) = \sum_{n=1}^{N} a_n h(t - t_n) \tag{4.6}$$

where $h(t)$ is the system impulse response. The impulse response of a reflected signal from the flat wood surface and its Fourier spectrum are shown in Figure 4.5a.and 4.5b.

4.2 Fourier Transform of Impulse Response

Assuming the Fourier transform of $s(t)$ is $S(\omega)$ or more generally,

$$F\{s(t - t_0)\} = e^{-j\omega t_0} S(\omega) \tag{4.7}$$

and applying this to two pulses separated in time by 2 t_0 we obtain display shown on a spectrum analyzer of:

$$|F\{s(t + t_0) + s(t - t_0)\}| = |e^{j\omega t_0} S(\omega) + e^{-j\omega t_0} S(\omega)| = |2\cos\omega t_0||S(\omega)| \tag{4.8}$$

Two pulses may result from two boundaries in the cherry tree. From Equation (4.8) the spectrum is now that of a single pulse modulated by $|2\cos\omega t_0|$ In other words, the envelope of the resulting spectrum is the same as that obtained for a single pulse, but the spectrum now has maxima and minima that depend on t_0.

Approximating the maxima of Equation (4.8) by the maxima of $|\cos\omega t_0|$ yields

$$\omega t_0 = n\pi, \quad n = 0, 1, 2, ...,\tag{4.9}$$

or

$$f_n = n/(2t_0) = n/(\Delta t)\tag{4.10}$$

where the f_n are the frequencies of the maxima and Δt is the total time delay between the two pulses.

Suppose now that the two incident signals are identical, except that the second has been shifted in phase by a constant amount φ with respect to the first. The spectrum, using Equation (4.7), becomes

$$F\{s(t+t_0) + s(t-t_0\pm\varphi)\} = \left|e^{j\omega t_0} + e^{\pm j\varphi}e^{-j\omega t_0}\right||s(\omega)|$$

$$= |2\cos(\omega t_0 \mp \varphi/2)||s(\omega)|\tag{4.11}$$

The resulting spectrum is thus identical to that expressed by Equation (4.8), except for a frequency shift equal to half the phase shift between the two incident signals. Equation(4.10) predicts that the maxima are separated by $1/(\nabla t)$ and occur at multiples of

$1/(\nabla t)$ Equation (4.11) predicts that the maxima are still separated by f_n, but that they no longer occur at multiples of $1/(\nabla t)$ but rather by:

$$f_n = \frac{n \pm \varphi/(2\pi)}{\Delta t} , \qquad n = 0, 1, 2, \dots \tag{4.12}$$

Thus, one can easily determine the phase shift between the two signals by first measuring $1/(\nabla t)$ and then solving for φ in Equation (4.12). The present result also explains the experimentally observed fact that the spectral maxima do not project back to zero frequency.

The differences in the time domain signal are exhibited by a difference in the spectral characteristics of the two signals. For a single frequency at a fixed spectral reference in a lossless, isotropic and homogeneous medium, the reflected signals from various boundaries are expressed as:

$$r(t) = \sum_{k=1}^{\infty} A_k \cos(\omega_0 t + \varphi_k) \tag{4.13}$$

where φ_k is the phase shift due to the respective time delay. A shift in the time domain by φ (φ positive corresponding to a time advance and φ negative to a time delay) corresponds in the frequency domain to multiplication of the Fourier transform by the linear phase factor $e^{-j\varphi}$ (Oppenheim and Schafer 1989).Therefore, the spectrum of the signal reflected from the first boundary is identical to the spectrum of the incident signal except

for a phase shift and amplitude reduction. Thus, the Fourier transform for the first reflected signal yields:

$$R(\omega) = A_1 \pi \left[e^{j\varphi_1} \delta(\omega - \omega_0) + e^{-j\varphi_1} \delta(\omega + \omega_0) \right] \qquad (4.14)$$

The term $e^{j\varphi_1}$ and $e^{-j\varphi_1}$ represent the phase shift due to the location of the reflecting surface.

For a non-borer-damaged sample, the reflected signal is:

$$r_n(t) = A_1 \cos(\omega_0 t + \varphi_1) + A_2 \cos(\omega_0 t + \varphi_2) \qquad (4.15)$$

where

φ_1 = time delay from the first boundary,

φ_2 = time delay from the bark-trunk interface,

A_1 = amplitude of the signal reflected from the first boundary, and

A_2 = amplitude of the signal received from the bark-trunk interface.

The spectrum of a signal reflected from the non-borer-damaged sample consists of two terms, the reflection from the surface of the cherry tree and from the bark-trunk boundary. This results in a sum of two signals with spectrum given by:

$$R_n(\omega) = A_1 \pi \left[e^{j\varphi_1} \delta(\omega - \omega_0) + e^{-j\varphi_1} \delta(\omega + \omega_0) \right] +$$

$$A_2 \pi \left[e^{j\varphi_2} \delta(\omega - \omega_0) + e^{-j\varphi_2} \delta(\omega + \omega_0) \right]$$

(4.16)

The Fourier transform of the reflected signal from non-borer-damaged sample is shown in Figure 4.6.

Similarly for a borer-damaged sample, the reflected signal consists of three terms: the reflection R [1] from the surface of the cherry tree, the reflection R [2] from the top of the damaged layer and the reflection R [3] from the bottom of the damaged layer. This results in a sum of three signals:

$$r_d(t) = A_{1d} \cos(\omega_0 t + \varphi_{1d}) + A_{2d} \cos(\omega_0 t + \varphi_{2d}) + A_{3d} \cos(\omega_0 t + \varphi_{3d}) \quad (4.17)$$

with spectrum given by:

$$R_d = A_{1d} \pi \left[e^{j\varphi_{1d}} \delta(\omega - \omega_0) + e^{-j\varphi_{1d}} \delta(\omega + \omega_0) \right] +$$

$$A_{2d} \pi \left[e^{j\varphi_{2d}} \delta(\omega - \omega_0) + e^{-j\varphi_{2d}} \delta(\omega + \omega_0) \right] +$$

(4.18)

$$A_{3d} \pi \left[e^{j\varphi_{3d}} \delta(\omega - \omega_0) + e^{-j\varphi_{3d}} \delta(\omega + \omega_0) \right]$$

where

φ_{1d} = time delay from the outer boundary,

φ_{2d} = time delay from the top of the borer-damaged layer,

φ_{3d} = time delay from the bottom of the borer-damaged layer,

A_{1d} = amplitude of the wave energy received from the first boundary,

A_{2d} = amplitude of the signal received from the top of the borer-damaged layer

and,

A_{3d} = amplitude of the signal received from the bottom of the borer-damaged

layer.

The Fourier transform of the reflected signal from the borer damaged is shown in Figure 4.7.

The above results apply to a single frequency. The same procedure can be applied to a range of frequencies to compose an arbitrary broadband signal.

In Figure 4.7 it is noted that the spectrum has well defined periodic spectral nulls. It is believed these due to frequencies interact with damage layer. Research is on going in this area and shows considerable promise. For example, the two main dips occurring approximately at frequency 1.5 and 2.2 megahertz in Figure 4.7 arise from the standing wave resonances of the boundaries to the damaged layer. They each appear as two main split dip because the damaged layer couple the standing wave in borer damaged sample to create an

up-shifted and a down-shifted resonance depending on whether the reflected signals from the bark surface and the bottom of the damaged layer are moving in-phase or out-of-phase. When the reflected signal is in phase case, the detected interface simply add some inertia to the motion and lower the frequency and its frequency spectrum in signal power compare with out of phase case. This phenomenon may be correlated signal from the interface between the bark and the trunk. When the reflected signal is out of phase case, the detected interface is stretched and compressed so that it adds stiffness to the motion and increases the frequency and its frequency spectrum decrease in the signal power.This phenomenon may be correlated to the reflected signal from damaged layer. In either case, the interface of sample are subjected to the stresses and can be expected to influence the numerical values at different frequencies. Therefore, this approach to detecting a borer damage is to compare numerical values of frequencies and its signal power.
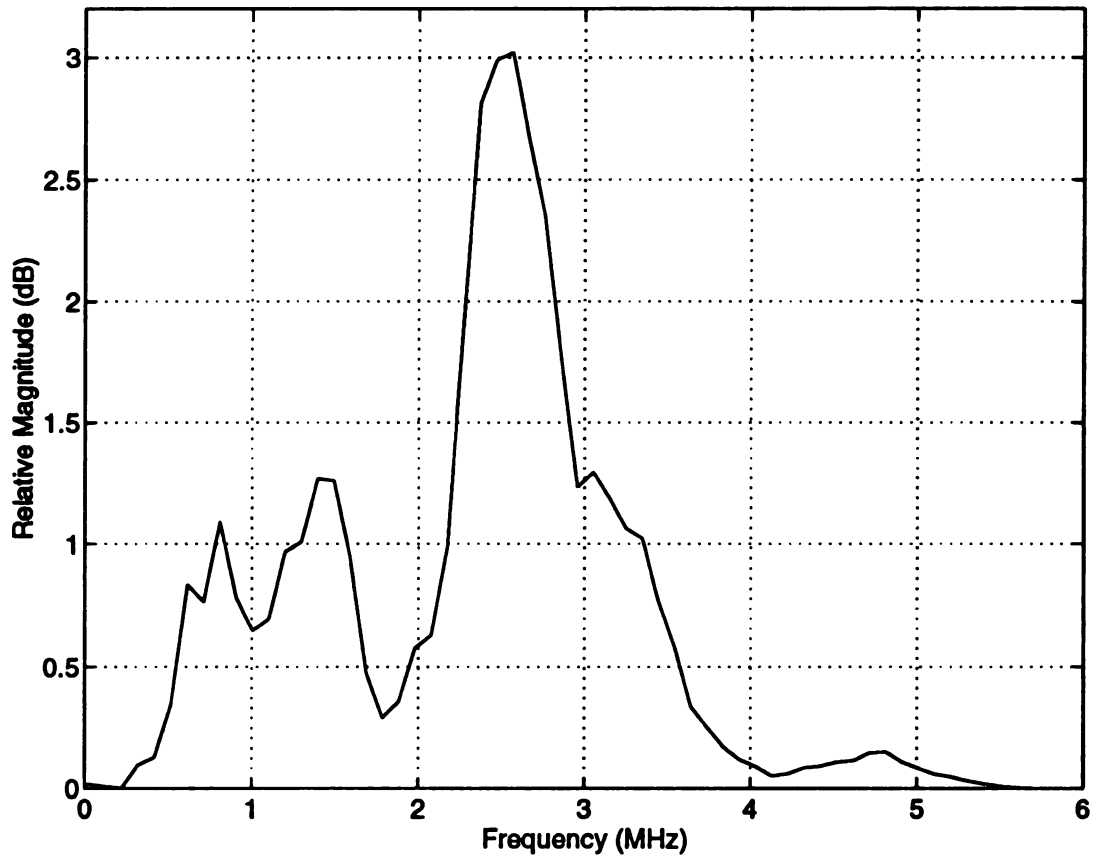
Figure 4.6 The Power Spectrum of the Reflected Signal from
a Non-Borer Damaged Sample
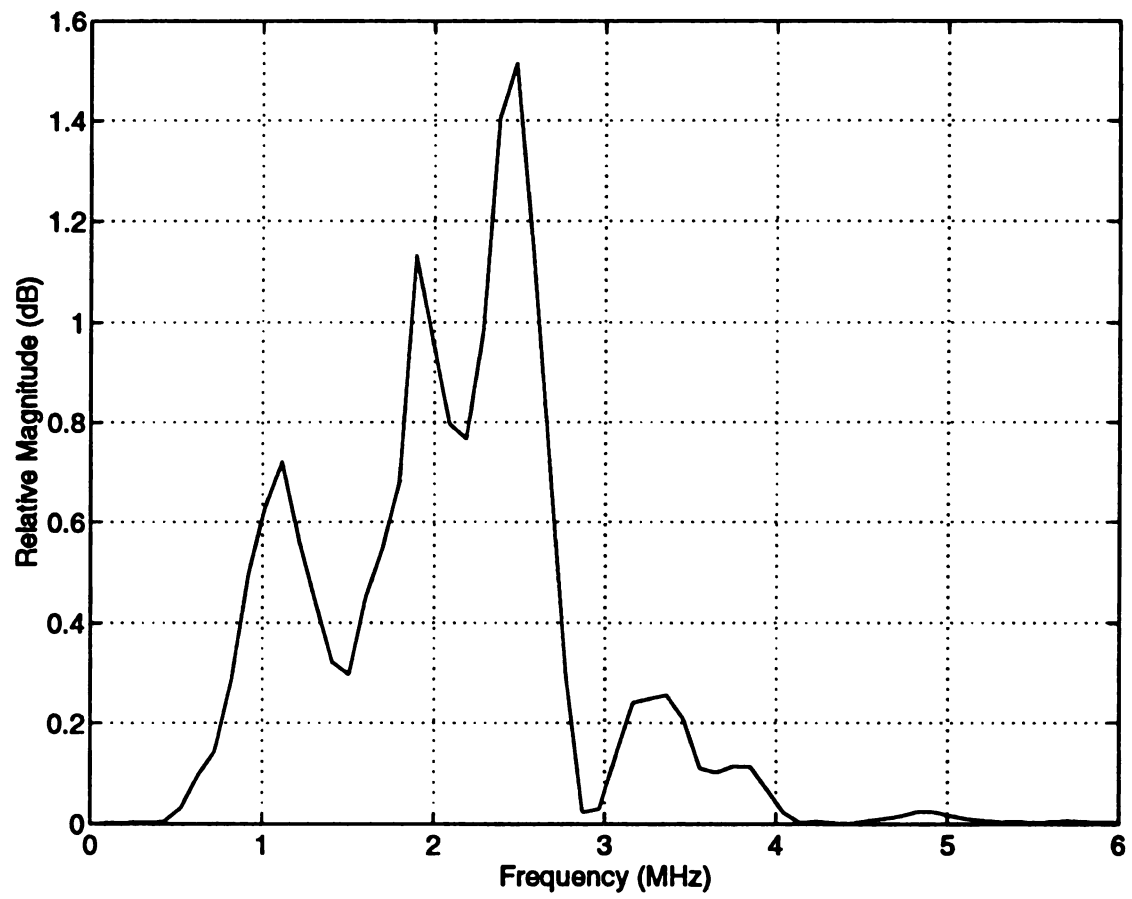
Figure 4.7 The Power Spectrum of the Reflected Signal from a Borer Damaged Sample

4.3 Gaussian-shaped Signals

One experimental technique commonly used by researchers is to measure the acoustic attenuation for highly attenuated materials using a Gaussian-shaped pulse. The effect of acoustic attenuation on an ultrasonic pulse having a Gaussian envelop is to translate the normalized power spectrum to lower frequencies by an amount ∇f, proportional to the attenuation α while maintaining the bandwidth. By applying this technique to identify the difference between borer and non-borer-damaged cherry tree have been obtained a good result. The borer damaged layer contains highly attenuated material relative to non-borer-damaged ones thus amplifying the spectrum translation. The attention coefficient α of a damaged layer can be estimated from the measured frequency translation experienced by the pulse power spectrum shift due to the propagation through the damaged layer.The difference between the borer and non-borer-damaged layer can be distinguished by comparing the amplitudes of the power spectra or the frequency shifts relative to their center frequencies. The experimental configuration for this measurement is shown in Figure 4.8.

The Transducer T/R transmits a wideband acoustic pulse into a water coupling medium and signal return is received by the same transducer. The output of the transducer is connected to a spectrum analyzer which computes the power spectrum of the received signal. The experiment is first performed with non-borer-damaged samples and then repeated with borer damaged samples. The schematic diagram illustrating reflections from this experiment and for the output spectrum as shown on a spectrum analyzer are provided in Figure 4.9a and in Figure 4.9b.
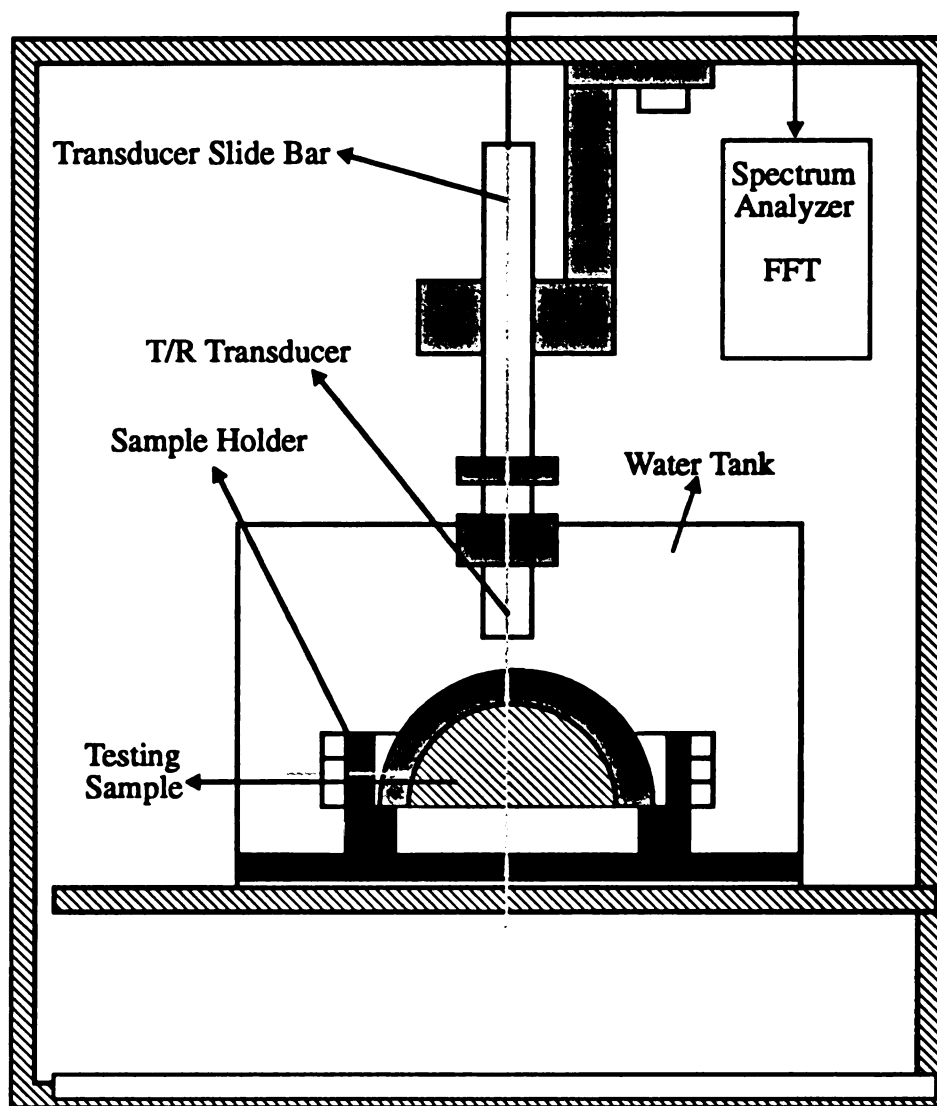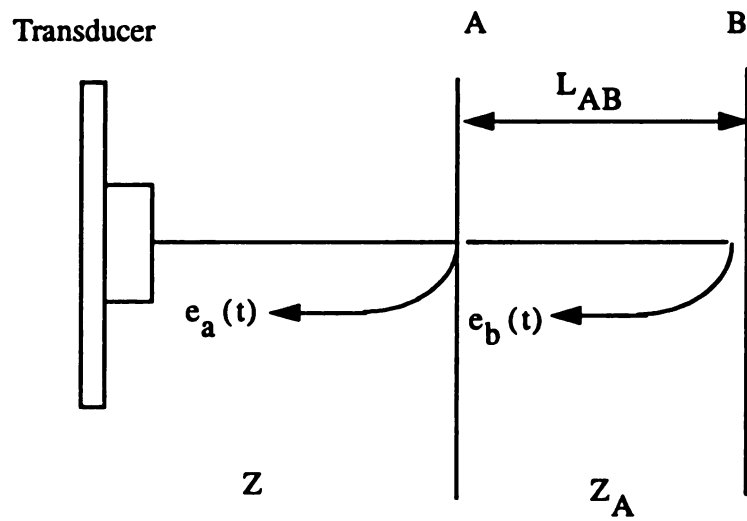
Figure 4.8 Experimental Configuration

Figure 4.9a Schematic Diagram Illustrating Reflections from a
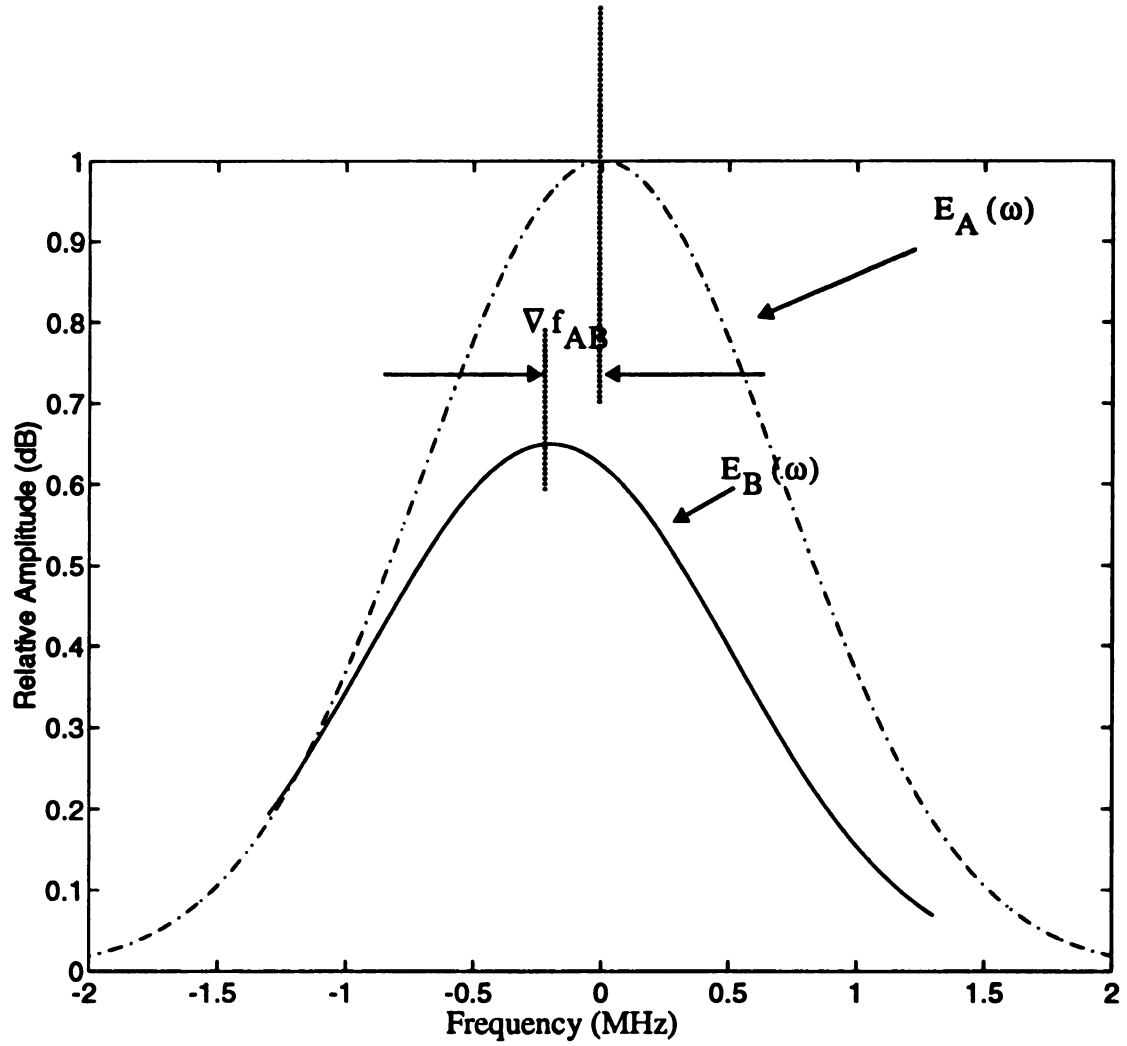Non-Borer-Damaged Sample

Figure 4.9b Illustration of Pulse Spectra Shifts due to Linear Attenuation of the Spectra of Reflected Pulses $E_A(\omega)$ and $E_B(\omega)$.

The theoretical model is described as follows:

The attenuation versus frequency characteristic, H (f) , of a frequency linear attenuating medium has the form $H(f) = \exp(-\kappa|f|x)$, where κ is a medium constant, f denotes frequency and x denotes the propagation distance. The Fourier transform of the output pulse, Y (f) , is $Y(f) = X(f)H(f)$, where X (f) is the Fourier transform of the input pulse. The center frequency shift of a Gaussian modulated pulse experienced by propagation through a distance x is determined as follows.

The Fourier transform of the incident Gaussian modulated signal is given by:

$$X(f) = (\pi/(2\sigma)) \times$$
$$\left[\exp\{-(\pi^2/\sigma^2)(f-f_0)^2\} + \exp\{(-(\pi^2/\sigma^2))(f+f_0)^2\}\right] \qquad (4.19)$$

The output Fourier transform Y (f) is then:

$$Y(f) = \exp(-\kappa xf)\exp\{-(\pi^2/\sigma^2)(f-f_0)^2\}$$
$$+ \exp(-\kappa xf)\exp\{(-(\pi^2/\sigma^2))(f+f_0)^2\} \qquad (4.20)$$

Completing the squares, a closed-form expression for Y (f) can be written in terms of

$$\hat{\sigma}^2 = \sigma^2 \qquad (4.21)$$

and

$$\nabla f = \hat{f}_0 - f_0 \qquad (4.22)$$

where $\hat{f}_0$ represents a shift downward in mean frequency of the pulse Fourier transform, f_0 is the center frequency and σ is the standard deviation of the Gaussian-shaped envelope.

Applying the above equations to damaged and non-damaged samples allow us to evaluate the attenuation corresponding to the center frequency shift of a Gaussian modulated pulse and thus to distinguish between the borer-damaged and non-borer-damaged samples. Figure 4.9a illustrates the reflections from non-borer-damaged samples. The spectrum, $E_A(\omega)$, of the echo from the first surface is:

$$E_A(\omega) = \rho_A P(\omega) \tag{4.23}$$

where ω is temporal frequency in radians and ρ_A is the pressure reflection coefficient and $P(\omega)$ denotes the spectrum of the pulse received from the surface of the cherry tree. $P(\omega)$ includes the effects of frequency dependent attenuation in coupling medium as well as transducer and transfer function. This function defines the frequency range over which valid data can be obtained.

For small values of ρ_A, the spectrum of the echo from the boundary between the bark and trunk is

$$B(\omega) = \rho_B P(\omega) e^{(-2\alpha l)/c} e^{(-j2\omega l)/} \tag{4.24}$$

where ρ_B is the reflection coefficient, l is the bark thickness, α and c are the absorptivity, nepers $((\mu s)^{-1}$, and propagation velocity, respectively. The ratio, $H(\omega)$, of the two spectra define in Equation (4.23) and (4.24) enable the desired parameters to be determined since $P(\omega)$ is removed from consideration:

$$(\omega) = (\rho_B/\rho_A)\,e^{-2\alpha T}e^{-j2\omega} \tag{4.25}$$

where $T = 1/c$

In most case, α is linearly proportional to ω and the ratio ρ_2/ρ_1 can be evaluated by interpolation to zero frequency. The phase of $H(\omega)$ specifies the phase relation between the two reflections which is ordinarily a linear function of frequency with a slope proportional to $1/c$. Therefore this function has the same form of $H(f) = \exp(-\kappa|f|x)$. By applying the same arithmetic methods, the borer damaged sample can be evaluated by the same procedures. The schematic diagram illustrating reflections for this experiment and the output of the spectrum analyzer using a borer-damaged specimen are shown in Figure 4.10a and 4.10b.
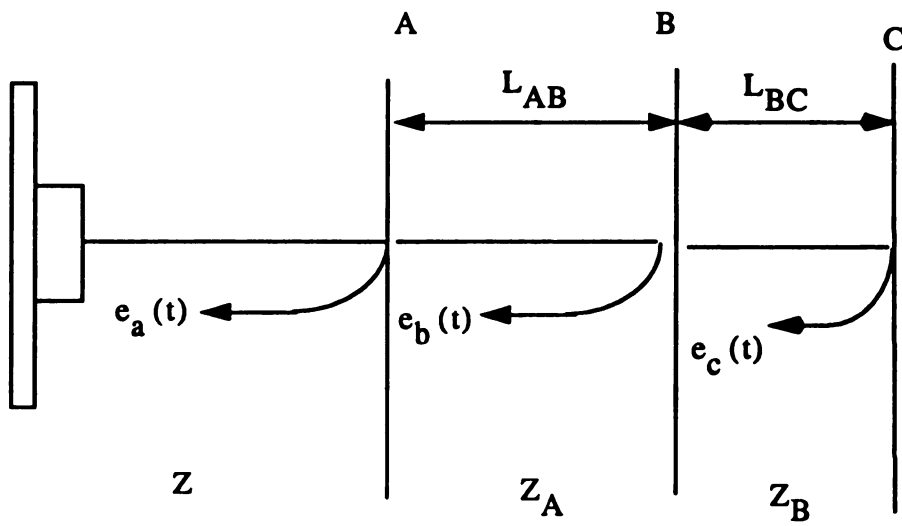
Figure 4.10a Schematic Diagram Illustrating Reflections From a
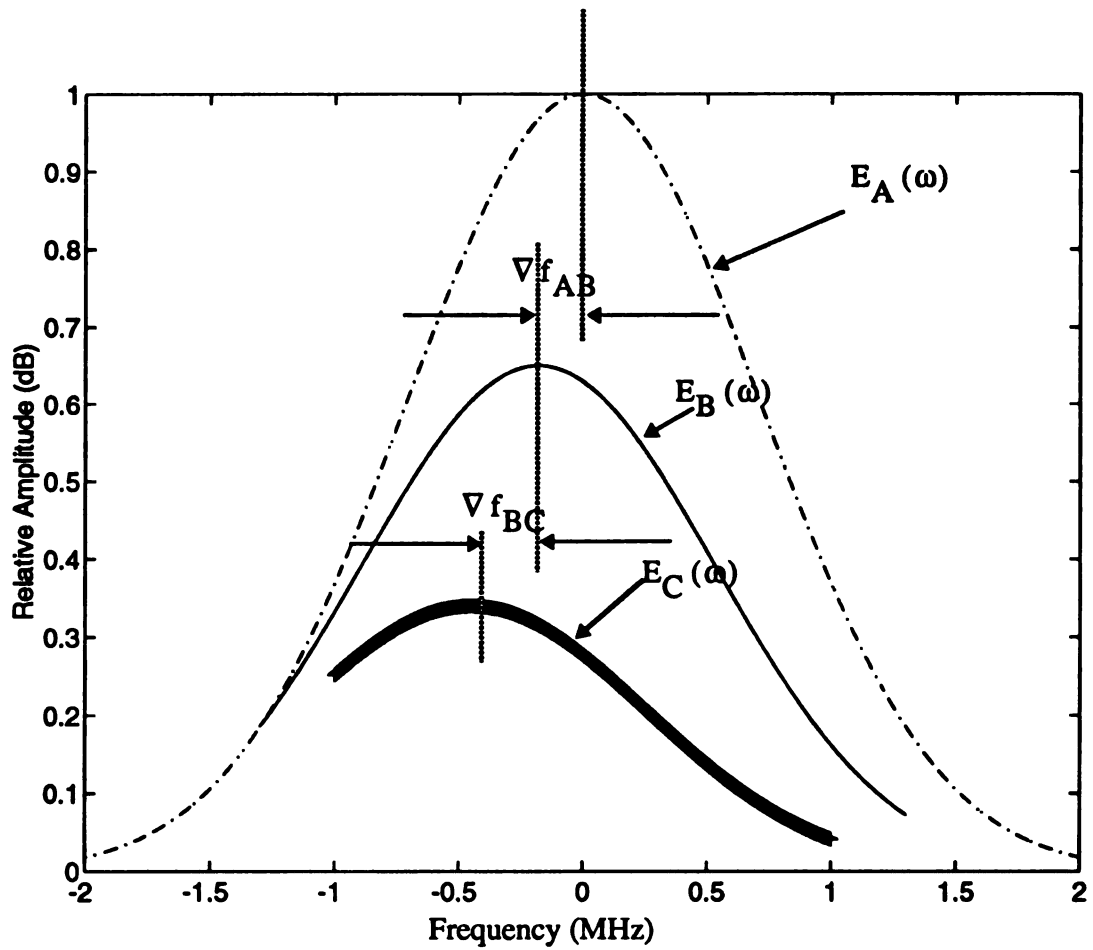Borer Damaged Sample

Figure 4.10b Illustration of Pulse Spectra Shifts due to Linear Attenuation in the Spectra of Reflected Pulses $E_A(\omega)$, $E_B(\omega)$ and $E_C(\omega)$.

5. EXPERIMENTAL RESULTS

The research reported here summarizes the results of using ultrasonic pulse-echoes to detect the borer damage inside cherry trees known to have been infested with borers. As the transducer is moved from non-borer-damaged to borer-damaged areas, the acoustic impedance decreases. The reflected signal R [1] from the non-borer-damaged samples (Figure 4.2.2a) had a higher acoustic impedance mismatch causing most of the energy to be reflected at the first boundary. In addition to the initial reflection, there were some low amplitude reflections caused by scattering from the surface roughness and wood anisotropy. The second reflection R [2] had a very low amplitude due to the highly attenuated bark and small acoustic impedance mismatch at the cambium between the bark and the undamaged trunk.

The reflected signal R [2] from a borer-damaged sample (Figure 4.2.3a),showed a high amplitude reflection at the interface between the bark and the borer-damaged layer caused by the high acoustic impedance mismatch at the interface. The amplitude of the third reflection, R [3] , was very small and overlapped with the reflection R [2] due to the very thin borer-damaged cambium layer. The differences between the received signals are more readily quantified if the frequency content of the reflected signals is determined. This is achieved by carrying out a Fourier transform of the reflected signal. The theoretical reflection amplitude versus frequency was obtained by programming the computer to calculate the frequency dependent reflection coefficient of a multilayer consisting of water, bark, damaged layer, trunk and water. The spectra of the reflected signals for non-borer-damaged and borer-damaged as shown in Figure 4.3 and 4.4 are combined in Figure 5.1. The

ultrasonic detection system can be used reliably to locate the borer-damaged areas when the frequency shifts between the non-borer-damaged and the borer-damaged samples are significant.It can also be used to find the extent of borer-damage by comparing the measured frequency shifts with those of sample containing known damage. The borer-damaged area has more energy in the returned pulse at low frequencies, but the energy content falls off rapidly with increasing frequency. The non-borer-damaged sample returned signal has a lower rate of decrease of energy with frequency. This means that the damaged area, consisting of feces, larvae and voids in the interface makes it is hard to pass the higher frequencies in the ultrasonic pulse.

The acoustic impedance difference between borer-damaged and non-borer-damaged samples from cherry trees caused a reflection coefficient difference. A comparison of the reflected signals from the two sample types showed that the acoustic impedance mismatch for the borer-damaged sample was larger than the acoustic impedance mismatch for the non-borer-damaged sample. Thus we essentially have identified a discriminant for borer damage detection. Table 1 summarizes the results of tests on 11 cherry tree samples which contained 5 borer-damaged and 6 non-borer-damaged samples. Comparison was done using time domain analysis and power spectral estimation. The results indicate that an extensive borer-damaged cherry tree sample can be identified by observing the first two reflected signals. The interference caused by the superposition of two signals of the same frequency with very little time delay. The phase difference causes a partial cancellation of the combined effects of reflected signal and determines which frequencies are out of phase and in phase. As a result, when the frequencies are out of phase, the frequency spectrum would exhibit a decrease in signal power at those frequencies and when the frequencies are in phase, the frequency spectrum could exhibit an increase in signal power at those frequencies. Thus, analysis of the spectrum composition or power at a given frequency pro-

vides the potential for distinguishing between borer-damaged and non-borer-damaged samples.

The experimental configuration is used to determine the central frequency shift as described in the previous section, except that rather than observing the signal reflected from different boundaries, the data is collected and analyzed automatically by an IBM-PC microcomputer. The entire reflected signal is divided into reflections from the sample surface, interface between bark and trunk and the damaged layer by locating the maxima in the reflected signal envelope and multiplying the reflected signals by an appropriate time window centered about the envelope maximum position. The power spectrum of each resulting section was calculated and frequency locations of the spectral maximum were noted. The frequency locations of power spectral maxima from the borer damaged sample are plotted in Figures 5.2 to 5.9 as a function of penetration depth into the cherry tree. In this data set the random variation of the spectral maxima locations due to boundary irregularities and the downward trend in the frequencies of spectrum due to attenuation can be observed.

For example, when a 5.2 cm bark width and 1.42 cm layer borer-damaged width are introduced into the acoustic path, the normalized received pulse power spectrum from the interface between the bark and trunk is shift downward by an amount $\nabla f = 0.06$ MHz from the central frequency of the pulse reflected only from surface of the cherry tree. The pulse spectrum from the damaged layer is shift downward an additional amount $\nabla f = 0.18$ MHz relative to the central frequency of the pulse from interface between the bark and the trunk. Thus their result shows that the application of these techniques to other insect damaged trees is highly promising.

6.CONCLUSIONS

The measurement of distinguishable features between borer-damaged and non-borer damaged cherry tree samples is still a difficult problem, but the results obtained demonstrate that there are characteristics in the ultrasonic signal, reflected by a borer-damaged structure, that provide information on the very thin damage layer at the interface between the bark and the trunk. The measurement of these features and their use in making predictions of the borer damage requires quantitative analysis of the signal and an excellent data base of signal returns from borer damaged and non-borer-damaged samples. This will allow reliable prediction of damage when comparison to the data base of borer damaged reference signals are made.

Excellent analysis and predictions on damage characteristics were possible using time domain and frequency domain techniques. The extension of frequency analysis to include the fine spectral details such as the periodic frequency dips referred to in the text would provide available additional material feature specification. This effort should be pursued
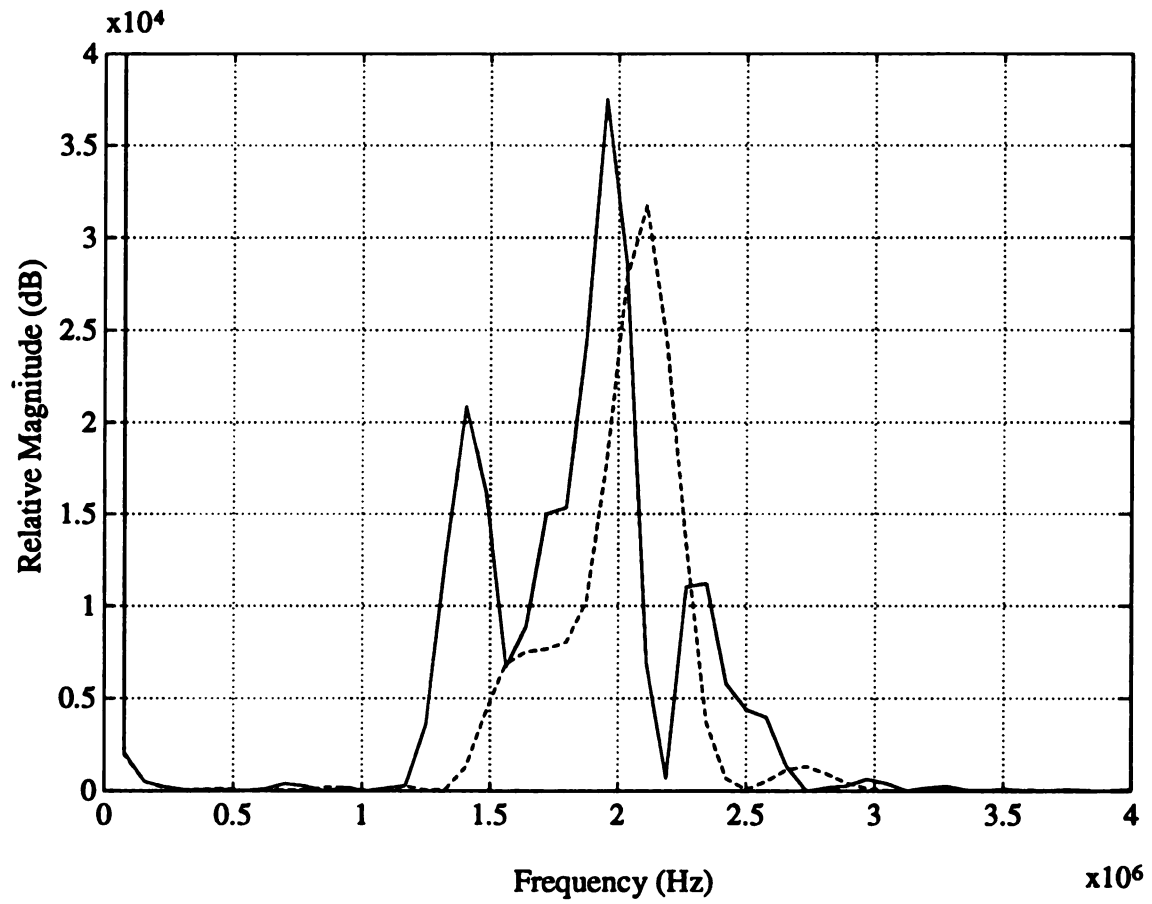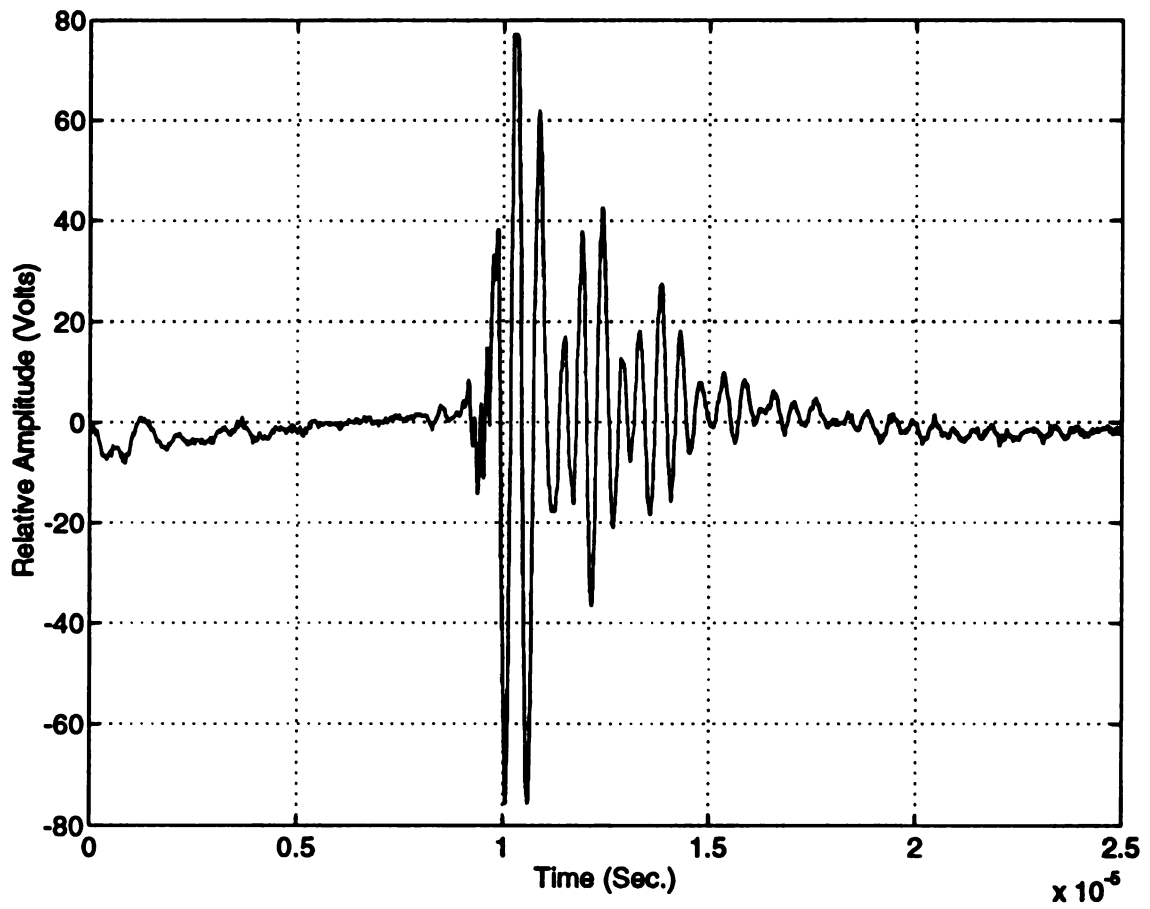
Figure 5.1 Power Spectrum Comparing Reflected Signals

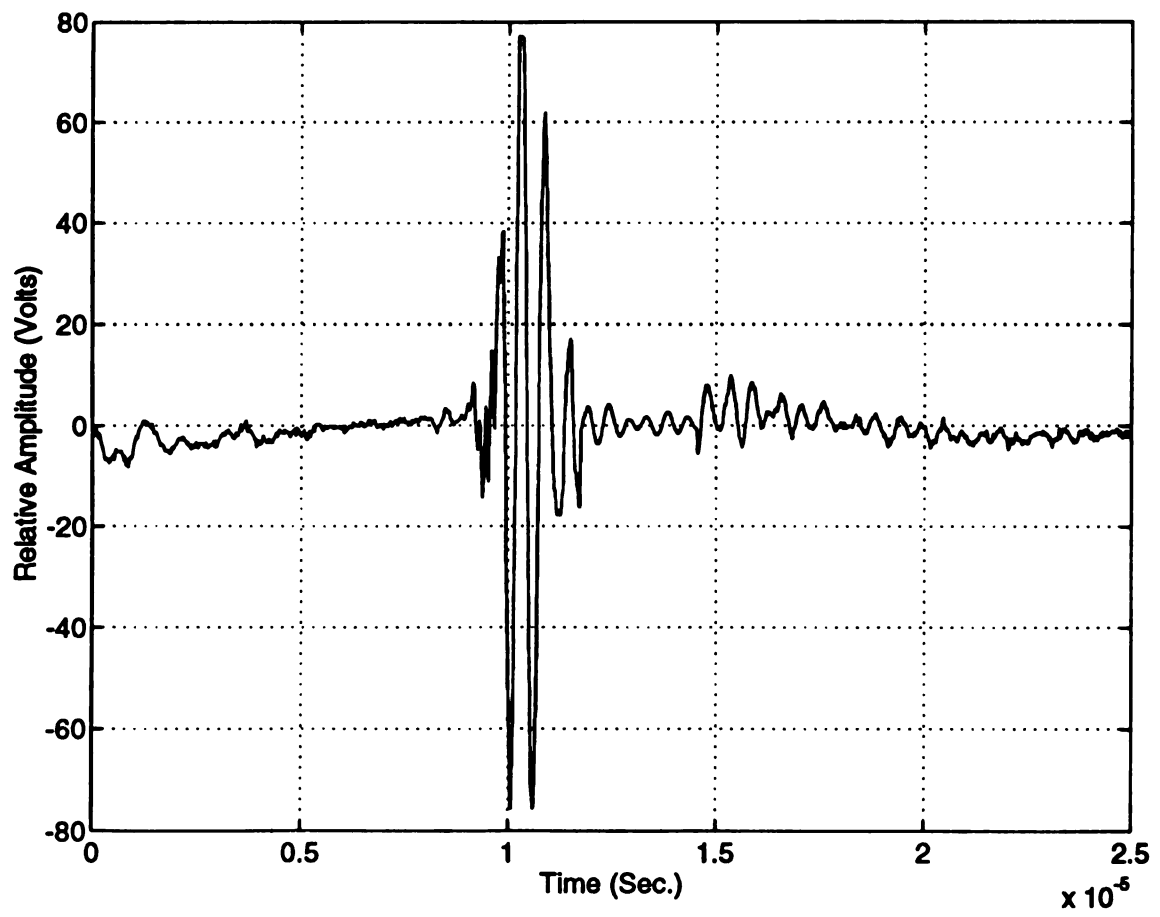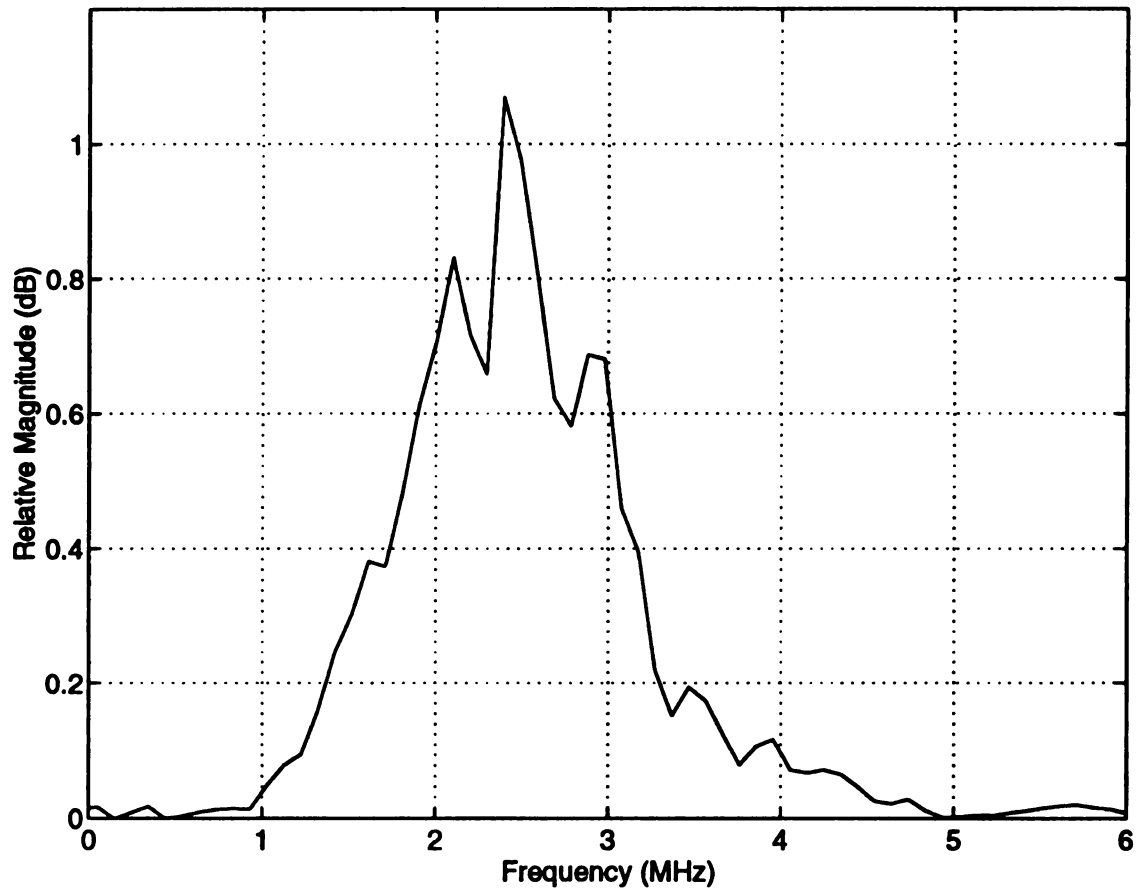Figure 5.2 The Overall Reflected Signal from a Bore Damaged Sample

Figure 5.3 The First Reflection from a Borer Damaged Sample

Figure 5.4 The Power Spectrum of the First Reflection from
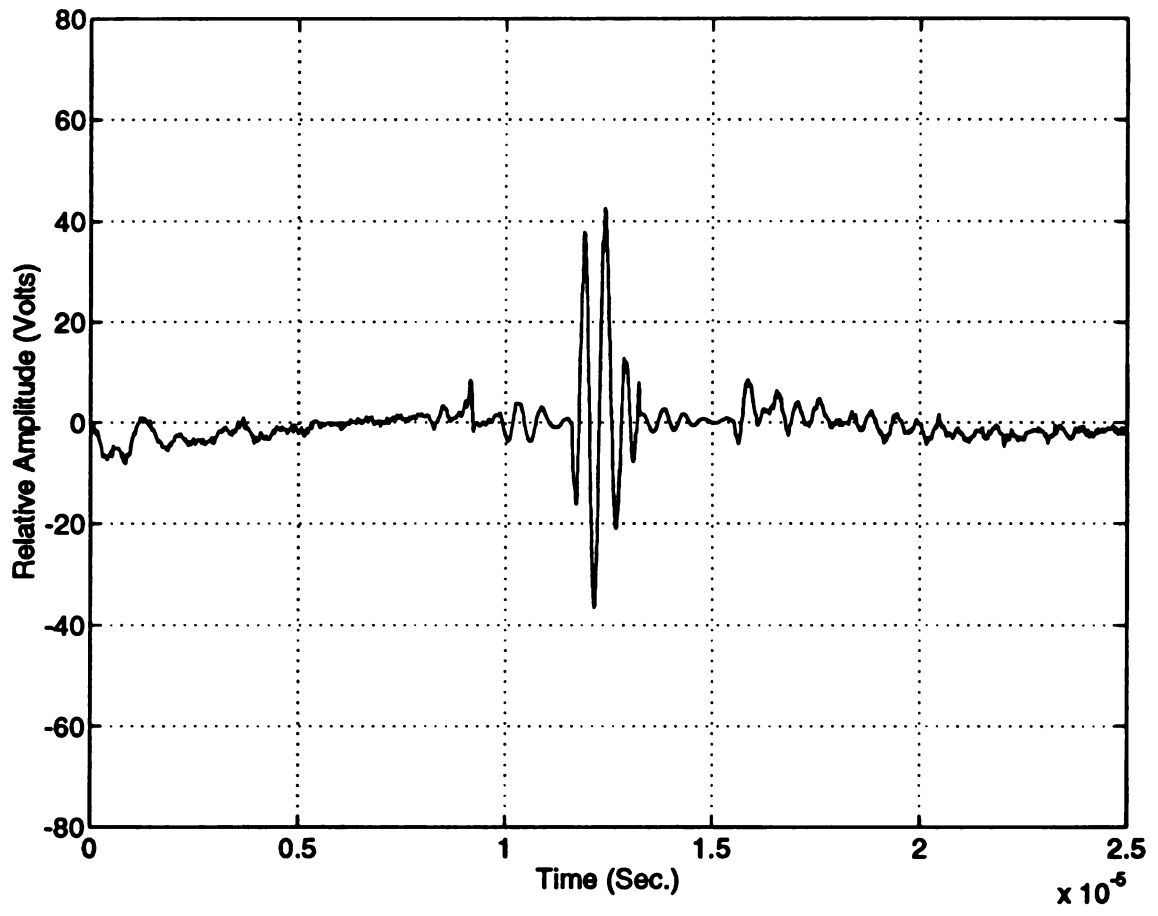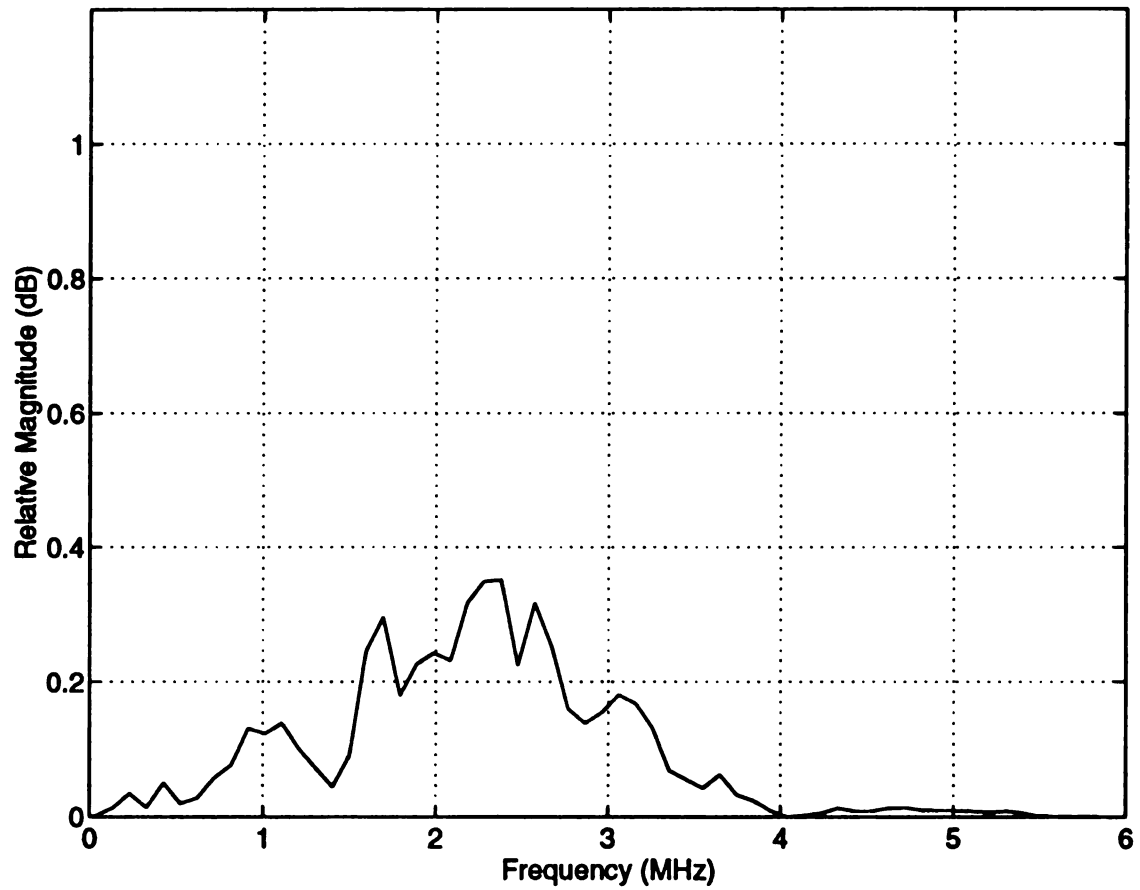the Surface of a Borer Damaged Sample

Figure 5.5 The Second Reflection from the Top of the Damaged Layer

Figure 5.6 The Power Spectrum of the Second Reflection
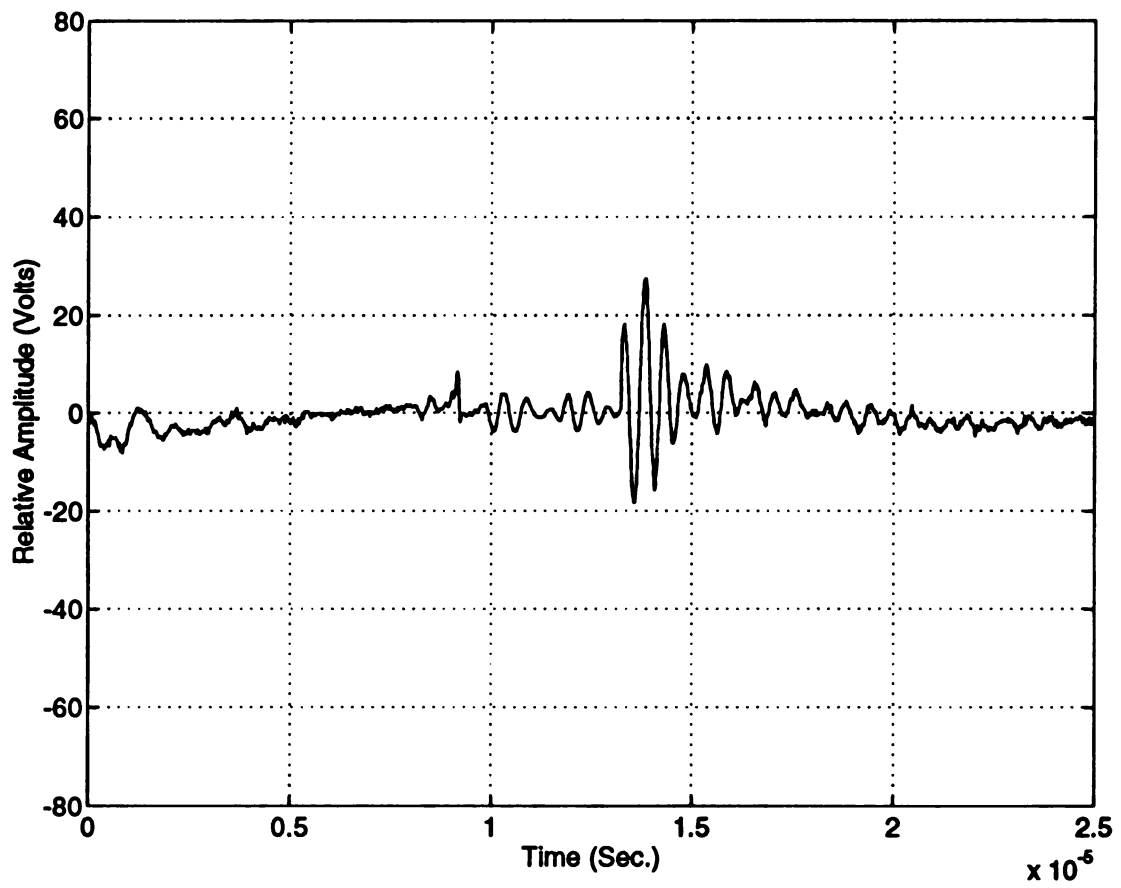from the Top of the Damaged Layer

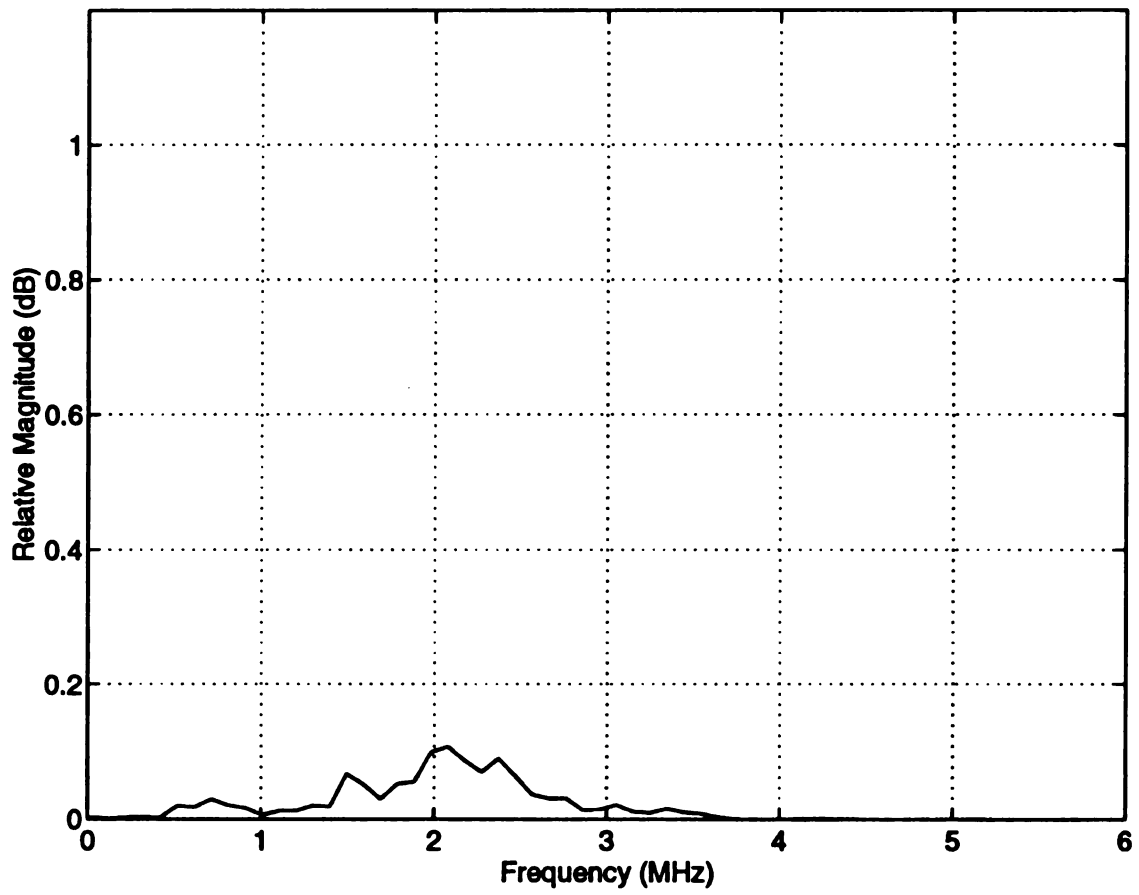Figure 5.7 The Third Reflection from the Bottom of the Damaged Layer

Figure 5.8 The Power Spectrum of the Third Reflection
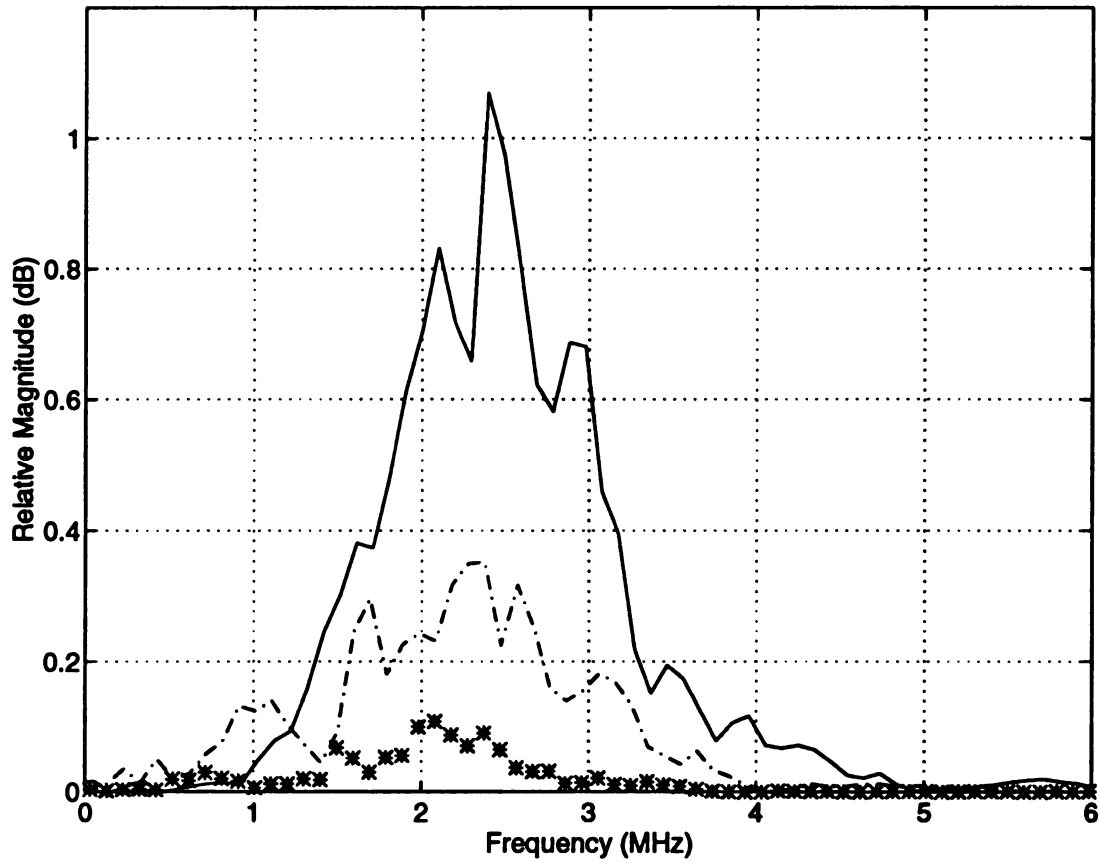from the Bottom of the Damaged Layer

Figure 5.9 The Power Spectra of All Reflections Superimposed Showing
the Frequency Shift due to Linear Attenuation

LIST OF REFERENCES

LIST OF REFERENCES

Alan V. Oppenheim, and Ronald W. Schafer. 1989. Discrete-Time Signal Processing, Prentice-Hall, Inc. A Division of Simon and Schuster Englewood Cliffs, NJ 07632.

Arita, K., and Kuratani, K. 1984.Wooden Pole Tester: For Determining the Strength of Decayed Poles, Japan Tele communications Review, Nippon Telegraph and Telephone Public Corp., Tokyo, Japan, pp 167-173 July,1984.

Carstensen, E.L. 1979. Absorption of Sound in Tissues, Ultrasound Tissue Characterization II. M. Linzer (Ed.). National Bureau of Standards, Spec Pub 525.

Chivers, R.C. 1980. Tissue characterization. Ultrasound in Medicine and Biology.

D.W. Hill, P. N. Well, and John P. Woodcock. 1977. Computers In Ultrasonic Diagnostics, Medical Computing Series. Vol, pp 35.

Edmonds, J. L. 1981. The Molecular Basis of Ultrasonic Absorption by Proteins. Ultrasound Med Biol.

F. C. Beall. 1988. Nondestructive Testing and Evaluation for Wood Products, Nondestructive Testing and Evaluation for Manufacturing and Construction. PP. 127-136.

Hayt, W. H. 1974. Engineering Electromagnets. McGraw-Hill Book Co., New York, New York.

Kuc, R., Schwartz, M., Von Micsky, L., Parametric estimation of the attenuation coefficient for soft tissue, Ultrasonic Symposium Proceedings, 1976.

L.Ferrari, J. P. Jones and Gonzalez, V. M. 1986. In vivo Measurement of Attenuation, IEEE Ultrasonics pp 66-71.

Lmaster, R. L., and Dornfeld, D. A. 1987. Preliminary Investigation of the Feasibility of Using Acousto-Ultrsonics to Measure Defects in Lumber. J. Acoust. Emiss. 6 (3): 157-165, 1987.

Miller, B. D., Taylor, F. L. and Popeck, R. A. 1965. A Sonic Method for Detecting Decay in Wood Poles, American Wood Preserves Association, From No. 1351.

M. J. Lighthill. 1958. Fourier Analysis and Generalized Functions, New York: Cambridge University Press.

Oppenheim, A.V. and A.S. Willsky. 1983. Signals and System. Prentice-Hall, Inc., Englewood Cliffs, New Jersey

Patton-Mallory, M., Anderson, K. D, and DeGroot, R. C. 1987. An Acousto-Ultrasonic Method for Evaluating Decayed Wood, Proceedings of Sixth Nondestructive Testing of Wood Symposium, Washington State University, Pullman, WA, pp. 167-189.

R. E. Edwards. 1967. Fourier Series: A Modern Introduction, Now York: Holt Rineheat and Winston, Inc.

Shaw, D. A. 1978. Bandpass Filter Comparator for Confirming the Absence of Serious Internal Voids in Wood Poles, IEEE Trans. Instrum. Meas. IM-27 (31).

Sample Dia.	Damage Extent	Reflected Signals Which are Detected		
7 cm	Extensive Damage (> 70%)	**R [1]**	R [2]	R [3]
9 cm	High Damage (> 50%)	R [1]	R [2]	R [3]
10 cm	Moderate Damage 25% < Damage < 50%	R [1]	R [2]	R [3] [1]
12 cm	Some Damage 10% < Damage < 25%	R [1]	R [2]	(NONE) [2]
14 cm	A Little Damage 2% < Damage < 10%	R [1]	R [2]	(NONE) [2]
7 cm	Non-Borer-Damage	R [1]	R [2]	(—) [3]
9 cm	Non-Borer-Damage	R [1]	R [2]	(—) [3]
10 cm	Non-Borer-Damage	R [1]	R [2]	(—) [3]
12 cm	Non-Borer-Damage	R [1]	R [2]	(—) [3]
14 cm	Non-Borer-Damage	R [1]	R [2]	(—) [3]
16 cm	Non-Borer-Damage	R [1]	R [2]	(—) [3]

Table Borer Damage Detection for Different Cherry Tree Diameters

and Damage Levels.

1. The reflected signal R [3] from the moderate damaged sample is very small and o·
; with R [2] . It is very hard to detect

2. The reflected signal R [3] from the a little damaged sample can not be detected du
y small borer tunneling.

3. No reflected signal R [3] in the Non-Borer-Damaged Samples.